

Session 1: High-frequency, small-scale oscillations and turbulence

Chairs: Sedina Tsikata and Ben Jorns

Panelists: A. Smolyakov, L. Wang, Y. Mikellides, E. Bello-Benitez, K. Hara



**ExB Plasmas
Workshop
2022**

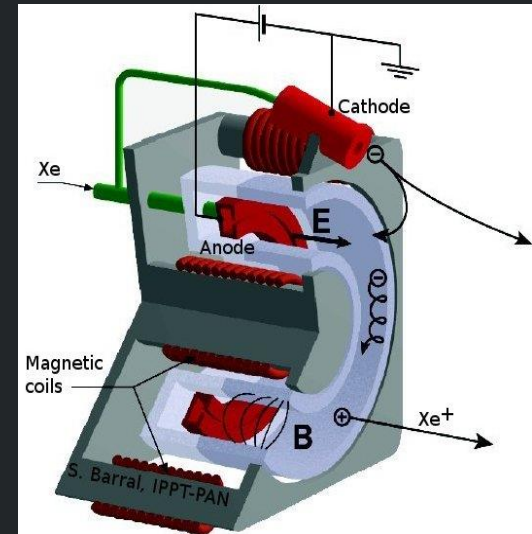
Madrid, online event

Context

- Anomalous electron transport is a feature of a range of magnetized plasmas
 - astrophysical plasmas (e.g. Earth's bow shock)
 - plasma pinches and other fusion devices (tokamaks, stellarators)
 - laboratory devices, such as Hall thrusters

$$D_{\perp} = \frac{\eta_{\perp} n \Sigma K T}{B^2}$$

classical mobility



- The observed mobility is found, across a very wide range of experiments, to scale differently

$$D_{\perp} = \frac{1}{16} \frac{k T_e}{e B}$$

Bohm mobility (semi-empirical)

Bohm, Massey and Burhop (1949)

- The Bohm mobility can exceed the classical mobility by as much as 4 orders of magnitude
 - one cause: unstable plasma waves *Yoshikawa and Rose, Phys. Fluids 1962*

Context

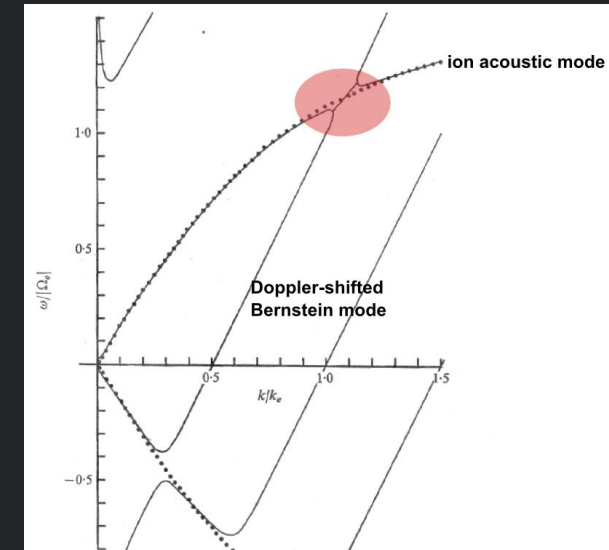
- Which types of waves are relevant for accounting for anomalous transport in thrusters?
 - a range of spatial and temporal scales present
 - short-scale, high frequency modes good candidates: strong wave-particle interaction expected
- This session focuses on findings relevant to high-frequency, small-scale oscillations
 - "high-frequency" – approaching or in MHz range
 - "small-scale" – electron Larmor radius scales (mm, sub-mm) to cm range
- The oscillations considered in this category include modes such as:
 - electron cyclotron drift instability (ECDI)
 - modified two stream instability (MTSI)
 - lower hybrid drift instability (LHDI)
 - ion-ion two stream instability (IITSI)
 - ion acoustic instability (IAI): not discussed in this talk

The electron cyclotron drift instability (ECDI)

Electron cyclotron drift instability (ECDI)

- Physical origin
 - fast relative particle drift (electron azimuthal drift in thrusters)
 - coupling of electron Bernstein and ion acoustic waves, with appearance of resonances
- Dispersion relation
$$1 + \frac{1}{k^2 \lambda_D^2} \left[1 + \frac{\omega - k_y V_d}{k_z v_{the} \sqrt{2}} e^{-\gamma} \sum_{m=-\infty}^{+\infty} Z(\zeta_m) I_m(\gamma) \right] - \frac{1}{2k^2 \lambda_{Di}^2} Z' \left(\frac{\omega - k_x v_i}{kv_{thi} \sqrt{2}} \right) = 0$$
 - conditions considered: electrostatic, magnetized electrons, unmagnetized ions
- This instability appears in several theoretical studies relevant to shocks, including:
 - Gary and Sanderson 1970, J. Plasma Phys. 4, 739 (1970)
 - Lampe et al., Phys. Fluids 15, 662 (1972)
 - Gary, J. Plasma Physics, 4, 753 (1970)
 - Forslund et al., PRL, 25, 1266 (1970); Forslund et al., PRL, 27, 1424 (1971);
Forslund et al, Phys. Fluids 15, 1303 (1972)
 - Wong, Phys. Fluids 13, 757 (1970)
 - Lampe et al, PRL 26, 1221 (1971); Lampe et al., Phys. Fluids 15, 662 (1972)
 - Lashmore-Davies, Phys. Fluids 14, 1481 (1970)

$$k_y V_d = n \omega_{ce}$$



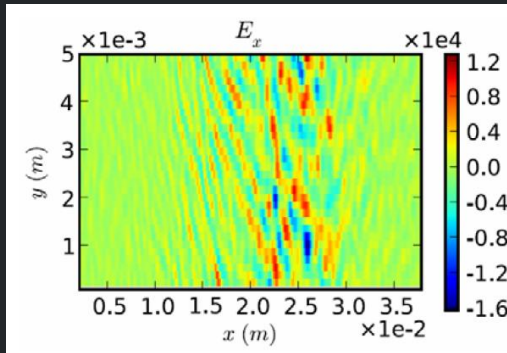
Gary and Sanderson (1970)
dispersion relation

Electron cyclotron drift instability (ECDI)

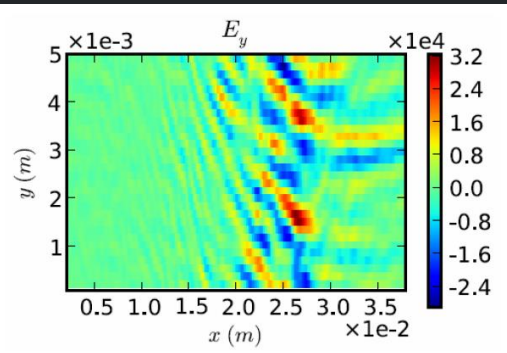
- In electric propulsion, the ECDI has been the focus of numerical and theoretical studies across several groups over the past ~15 years:
 - Adam, Héron and Laval Phys. Plasmas **11**, 295 (2004)
 - A. Ducrocq, PhD thesis, Ecole Polytechnique (2006)
 - Héron and Adam, Phys. Plasmas 20, 082313 (2013)
 - Cavalier et al. Phys. Plasmas 20, 082107 (2013)
 - Coche and Garrigues, Phys. Plasmas 21, 023503 (2014)
 - Katz et al, IEPC-2015-402 (2015)
 - Lafleur et al., Phys. Plasmas 23, 023502 (2016)
 - Lafleur et al., Plasma Sources Sci. Technol. 26, 024008 (2017) ; 2018
 - Janhunen et al, Phys. Plasmas 25, 082308 (2018)
 - Boeuf and Garrigues, Phys. Plasmas 25, 061204 (2018)
 - Taccogna et al., Plasma Sources Sci. Technol. 28, 064002 (2019)

Electron cyclotron drift instability (ECDI)

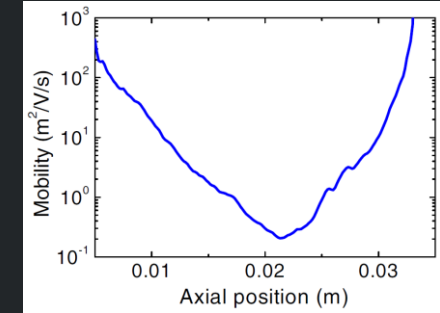
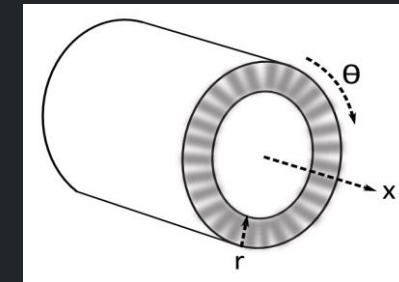
- In simulations: appearance of an azimuthal electric field in region of where turbulence-driven mobility is expected to dominate



axial component of mode E field

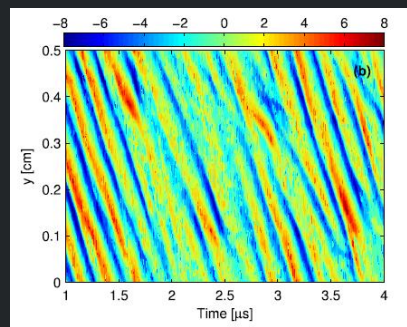


azimuthal component of mode E field

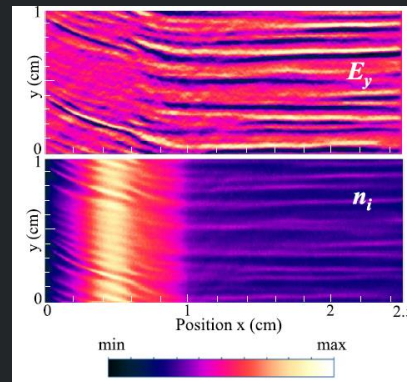


Adam et al., Plasma Phys. Control. Fusion 50, 124041 (2008)

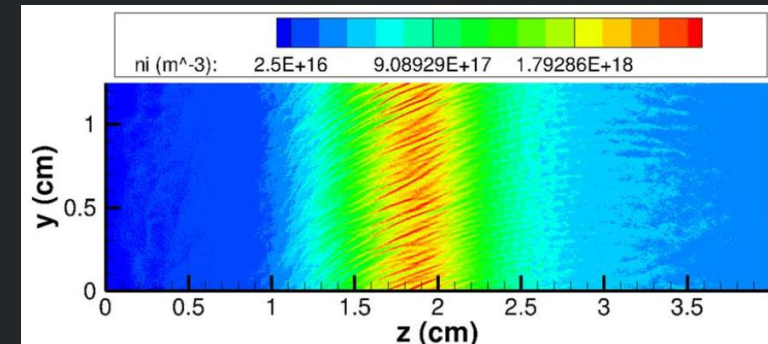
$$\mu_{\perp} \approx j_{ex}/e n_e E_x$$



Lafleur et al, Phys. Plasmas 23, 053502 (2016)



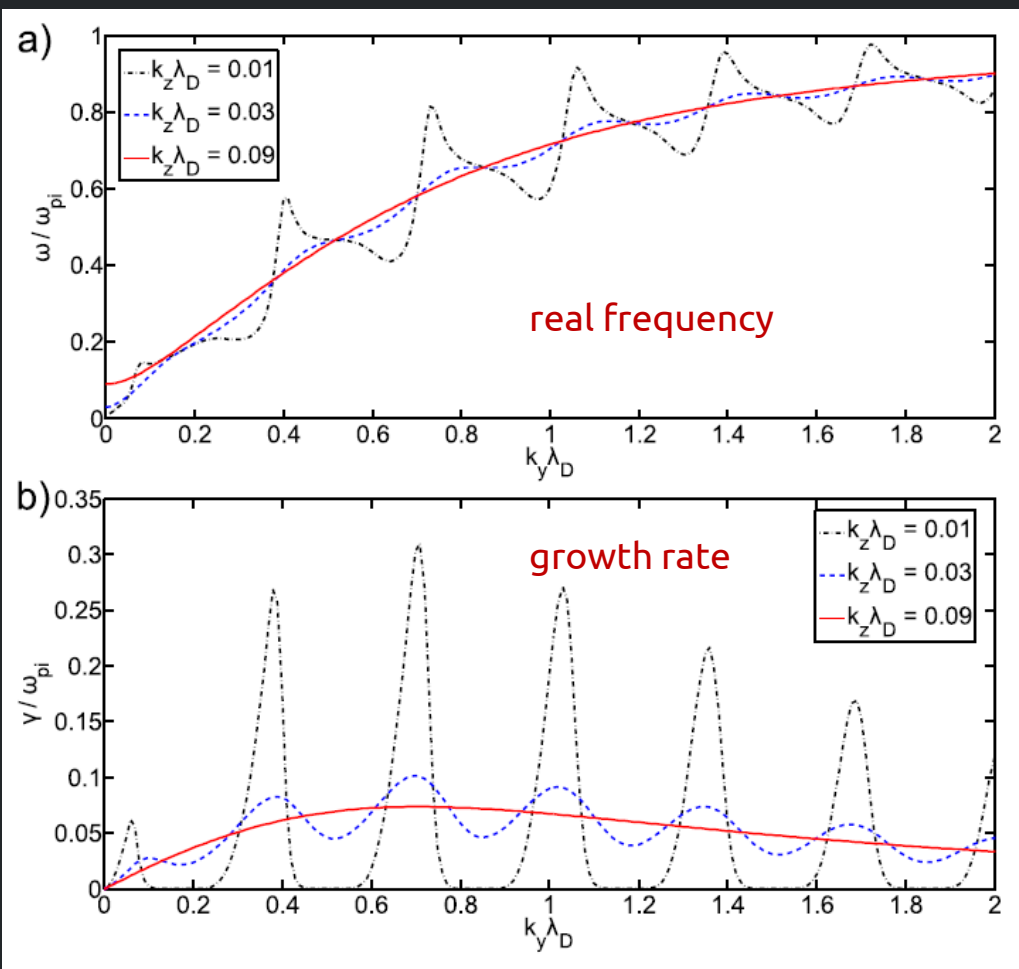
Boeuf and Garrigues, Phys. Plasmas 25, 061204 (2018)



Taccogna et al., Plasma Sources Sci. Technol. 28 (2019) 064002

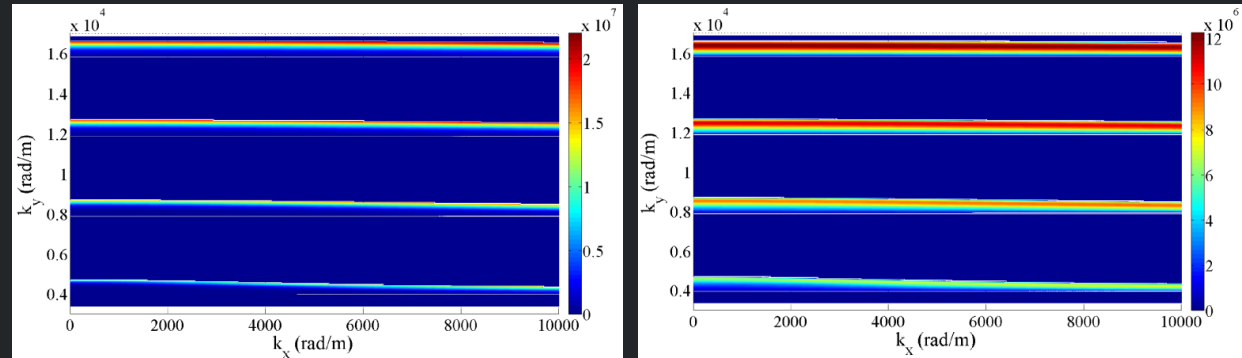
Electron cyclotron drift instability (ECDI)

- In linear kinetic theory: discrete mode

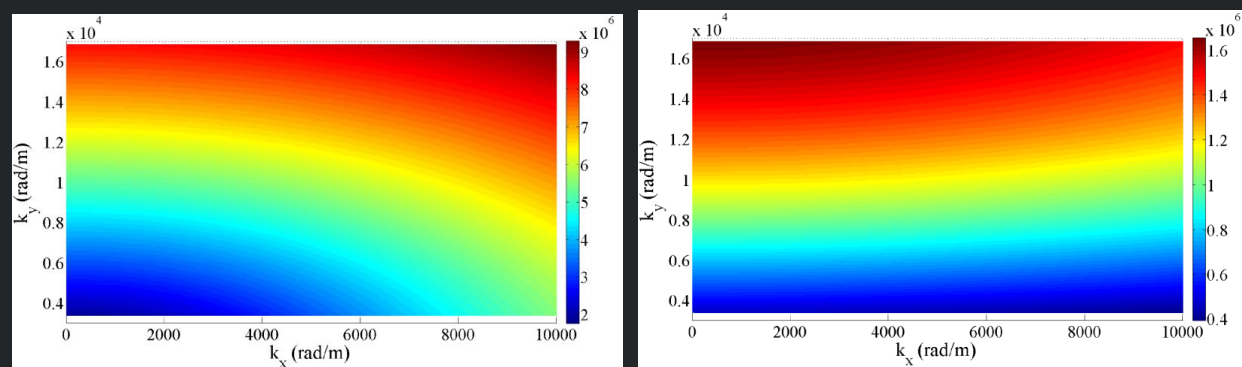


Cavalier et al. Phys. Plasmas 20, 082107 (2013)

2D: frequency and growth rate



3D: frequency and growth rate
(inclusion of radial wave vector)



Tsikata, PhD thesis (2009)

Electron cyclotron drift instability (ECDI)

- Open question: how exactly does this wave intervene in transport?

$$m_e n_{e0} \frac{D}{Dt} [\vec{V}_e] + \nabla P_e - e n_{e0} (\vec{E}_0 + \vec{V}_e \times \vec{B}) = -\nu_{ce} m_e \vec{V}_e + e n_e \vec{S}_e$$

Katz et al, IEPC-2015-402 (2015)

$$\vec{S}_e = \frac{1}{n_{e0}} \int \langle \vec{E}_1 f_{e1} \rangle dV^3$$

$$j_{ez} = \frac{e^2 n_{e0}}{m_e \nu_{ce} (\Omega_e^2 + 1)} [E_{0z} + S_{ez} - \Omega_e S_{e\theta}]$$

current density across B

$$\nu_{AN} = \left[\frac{e}{n_{e0} m_e} \right] \left[\frac{B}{E_{0z}} \right] \sum_k \gamma_k k N_k$$

turbulence-induced mobility is a function of wave action density N_k and mode growth rate

effective drag of plasma turbulence on bulk parameters

Lafleur et al., Phys. Plasmas 23, 023502 (2016): ECDI as the source of enhanced electron-ion friction force

$$\mu_{\text{eff}} = \frac{\nu_{ez}}{E_z} = \frac{\frac{|q|}{m \nu_m}}{1 + \frac{\omega_{ce}}{\nu_m^2}} \left[1 + \frac{\omega_{ce}}{\nu_m} \frac{R_{ei}^{\text{IE}}}{|q| n_e E_z} \right].$$

Electron cyclotron drift instability (ECDI)

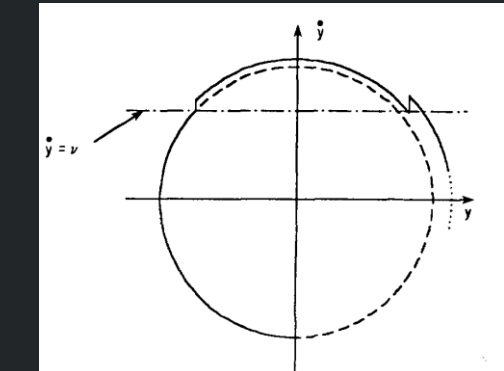
- Open question: how exactly does this wave intervene in transport?
 - possible interaction mechanism analogous to ion heating by a lower hybrid wave
C. F. F. Karney, Phys. Fluids 21, 1584 (1978)
 - provided resonance condition between the wave and particle (ion) is met, energy transfer from the wave can occur

$$\omega = \vec{k} \cdot \vec{v}$$

- net effect = a deviation in particle trajectories, and stochastic particle motion
- this mechanism was evaluated for the Hall thruster context by A. Ducrocq, PhD thesis, Ecole Polytechnique (2006)

how is this condition satisfied?

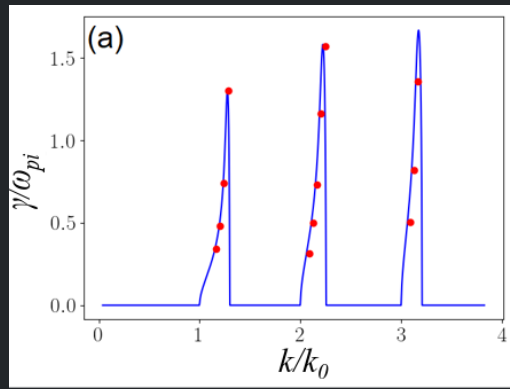
wave frequency in the electron reference frame: $\omega_d = \omega - k_y V_d$
for energy transfer: $\omega_d \gg \omega_{ce}$
eg. for $\omega = 5 \text{ MHz}$ ($31 \times 10^6 \text{ rad/s}$), $k_y = 4000 \text{ rad/m}$, $V_d = 7 \times 10^5 \text{ m/s}$,
 $\omega_d \sim 2.8 \times 10^9 \text{ rad/s}$, while $\omega_{ce} = 2.6 \times 10^9 \text{ rad/s}$



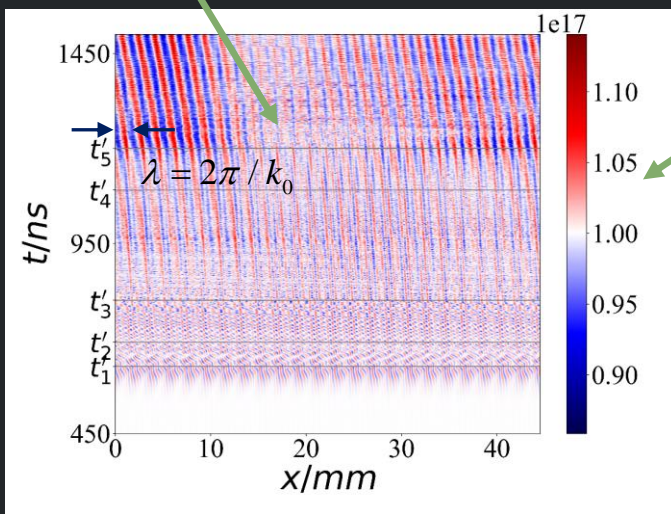
Discussion of new studies

Results from some recent articles on the ECDI will be discussed in this session:

- *Nonlinear regimes of the electron cyclotron drift instability in Vlasov simulations (2021)*
A. Tavassoli, A. Smolyakov, M. Shoucri, R. Spiteri, University of Saskatchewan
[arXiv:2112.12221](https://arxiv.org/abs/2112.12221)
- *Electron cyclotron drift instability and anomalous transport: two-fluid moment theory and modeling (2021)*
Liang Wang, Ammar Hakim, Bhuvana Srinivasan, James Juno
[arxiv:2107.09874](https://arxiv.org/abs/2107.09874)



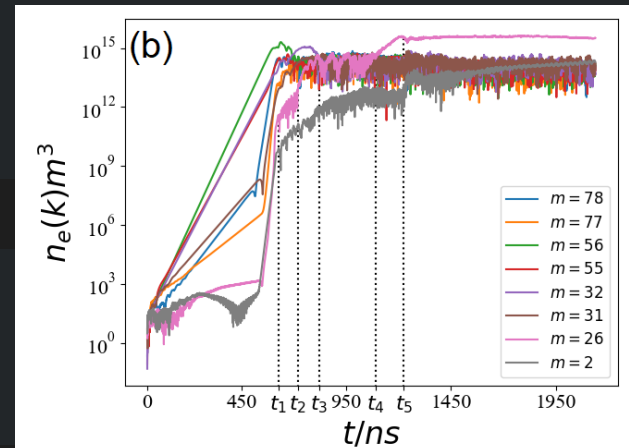
Long wavelength mode,



Growth rates from simulations (red) and linear kinetic theory (blue)

Several nonlinear mode transitions

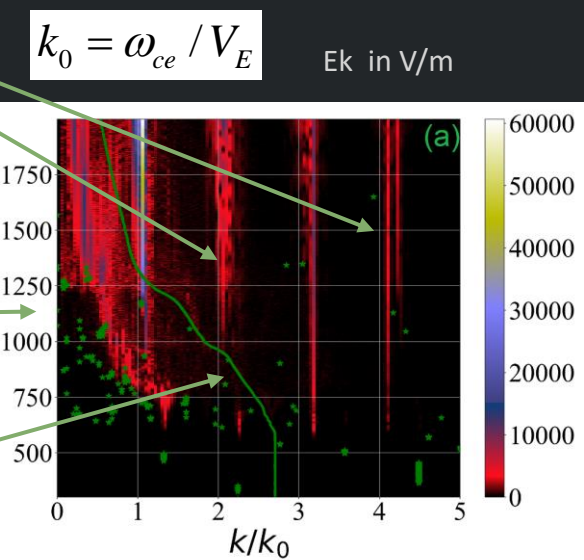
One-dimensional Vlasov simulations of ECDI in conditions similar to previous PIC simulations (Janhunen et al, PoP 2018). Applied axial electric field, no virtual axial length

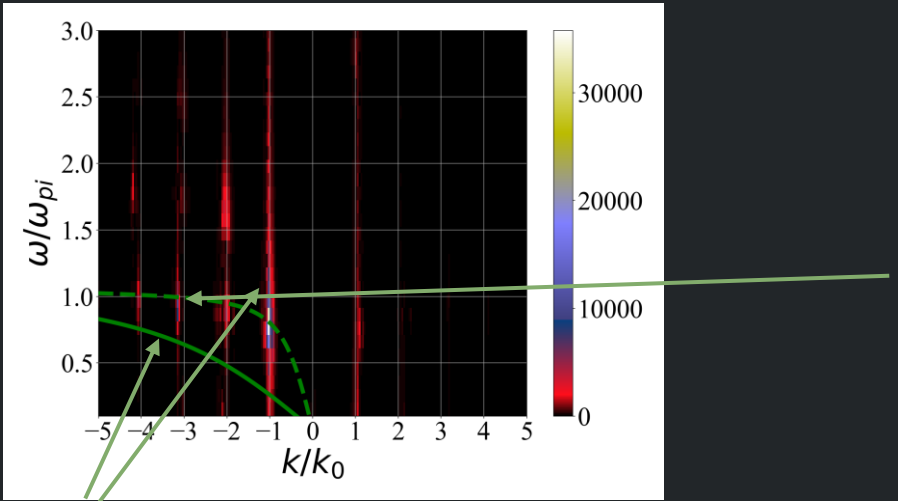


Cyclotron resonances are most unstable, followed by inverse cascade to the saturation

At saturation the dominant modes are well below of the "ion sound mode"

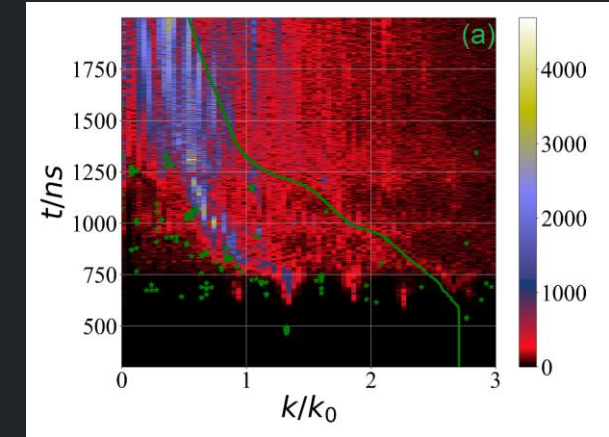
Evolution of the "ion sound wavelength"





“Ion sound” dispersion for initial and final Te

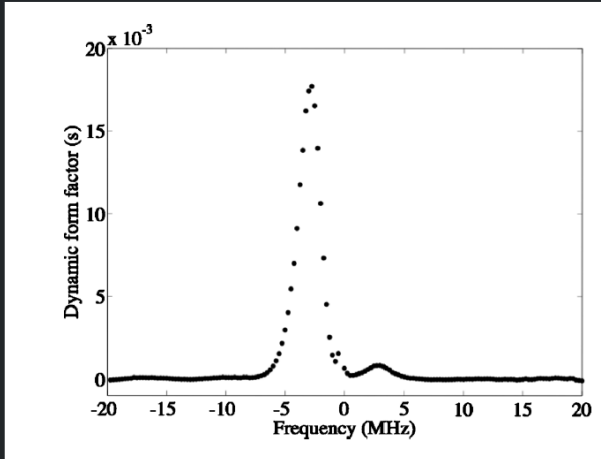
- Strong inverse cascade in the spectrum of nonlinear (axial, anomalous) current
- Ion sound (ω_{pi}) features are weak



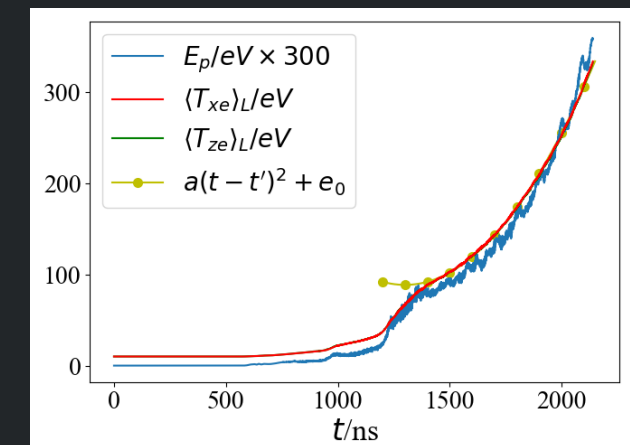
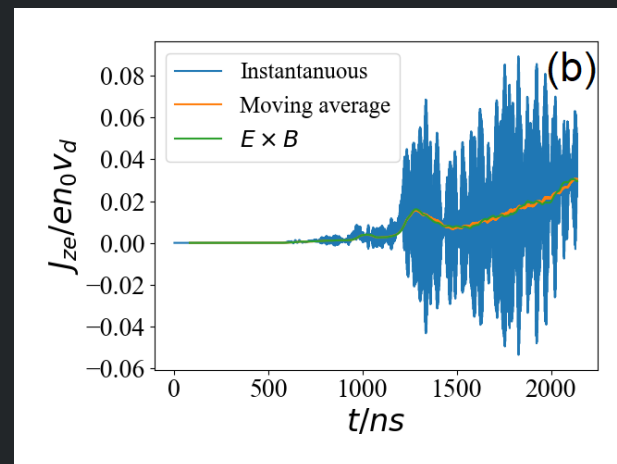
Average anomalous current follows $\langle \tilde{n} \tilde{E} / B \rangle$

Strong heating, similar to PIC (artefact of 1D)

Backward wave, in the direction opposite to azimuthal drift, supported by observations from CTS experiments



Tsikata et al, Phys. Plasmas 17, 112110 (2010)



Conditions

- 1D electrostatic modes
- 1D two-fluid plasma with fully magnetized electrons and unmagnetized ions
- background magnetic field B_0 along z
- wavevector k along x, perpendicular to B_0
- background electric field $E = E_0$ along y
- fully magnetized electrons flow at the $E \times B$ drift velocity along x

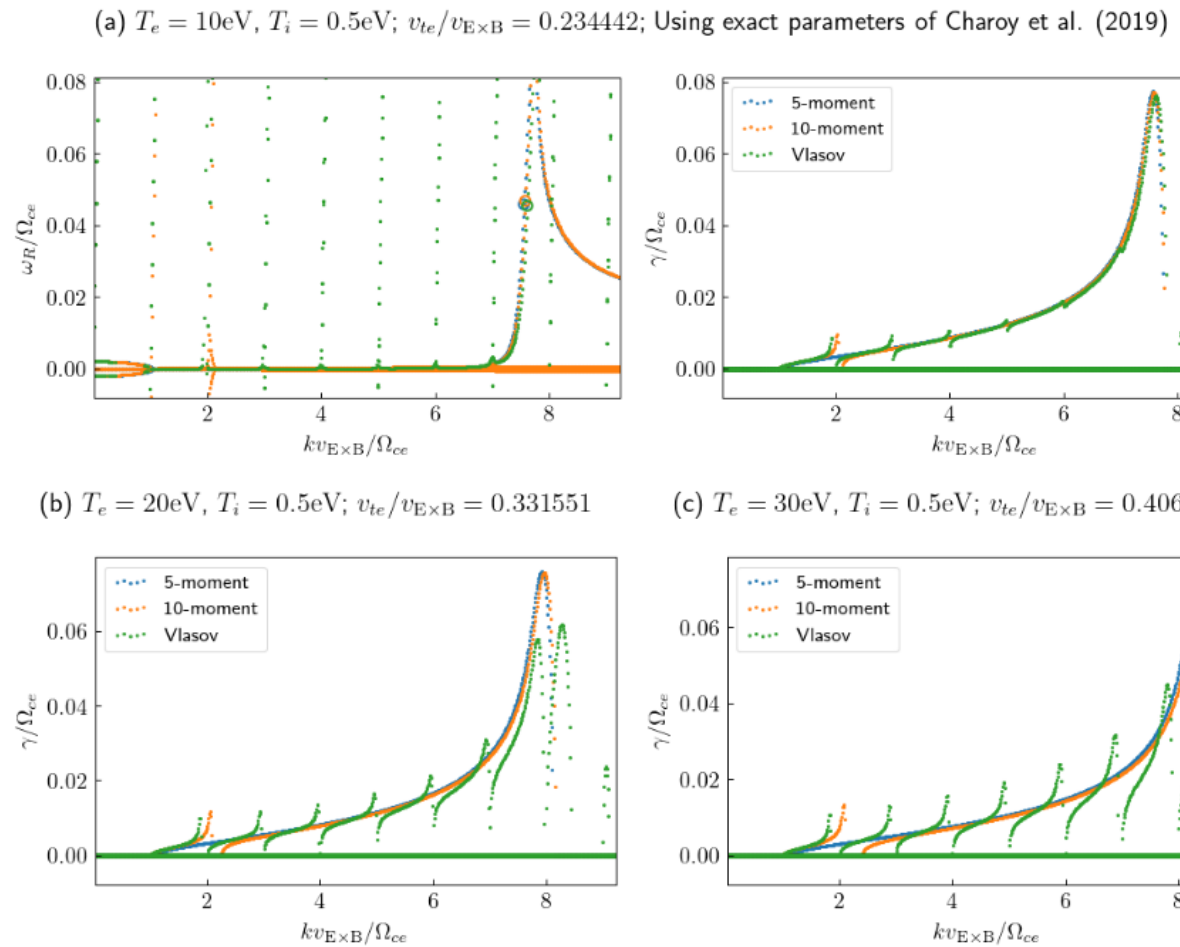
- The dispersion relation in the 5-moment regime can be written as

$$1 = \frac{\omega_{pi}^2}{\omega^2 - k^2 c_{si}^2} + \frac{\omega_{pe}^2}{(\omega - kv_{E \times B})^2 - k^2 c_{se}^2 - \Omega_{ce}^2}$$

- 5-moment and 10-moment dispersion relations solved

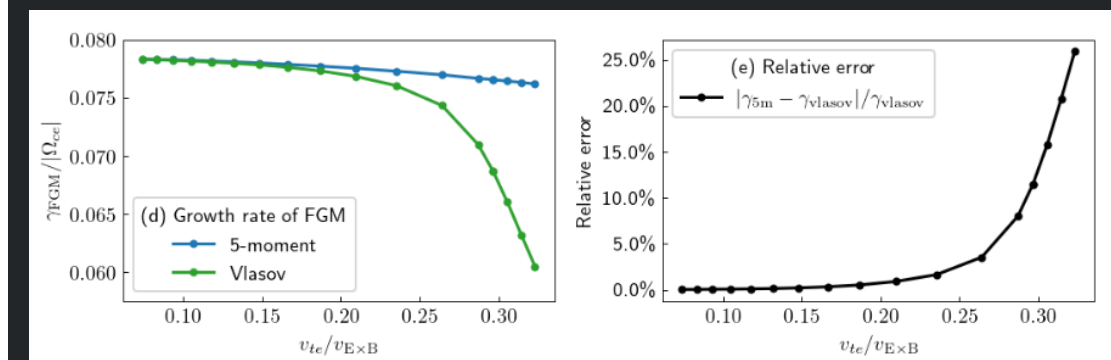
<https://arxiv.org/abs/2107.09874>

Electron cyclotron drift instability and anomalous transport: two-fluid moment theory and modeling
 Liang Wang, Ammar Hakim, Bhuvana Srinivasan, James Juno

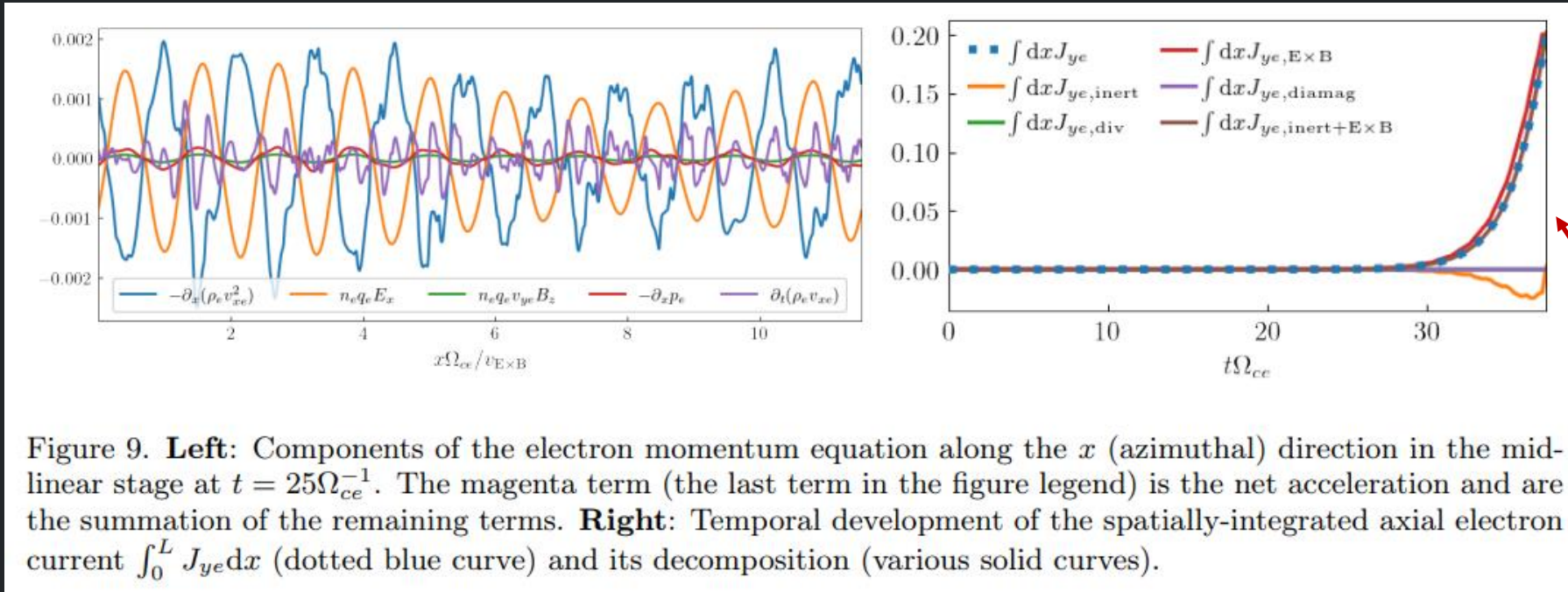


parameters from benchmark paper:

Charoy et al., Plasma Sources Sci. Technol. 28 (2019) 105010 (17pp)



similarity between solutions obtained for 5- and 10-moment models and Vlasov case



Overall:

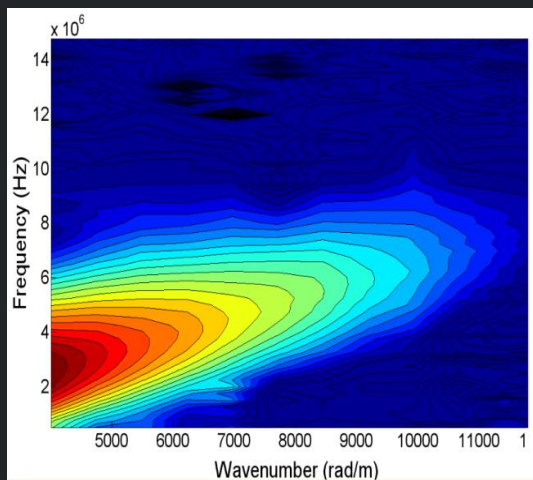
- evidence that ECDI-like mode can develop in a collisionless two-fluid plasma

Questions to reflect on: ECDI

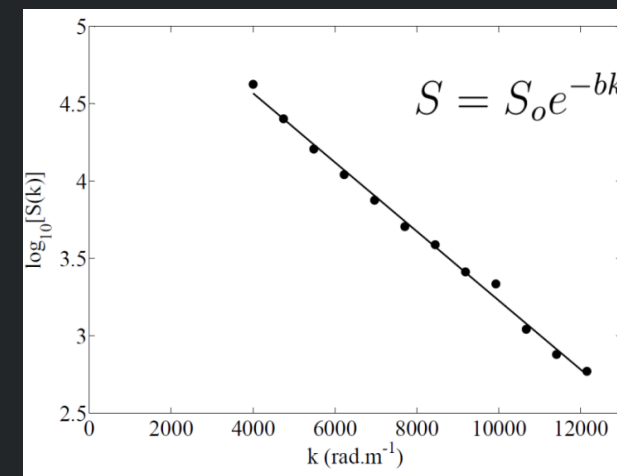
- Multiple simulations show an unambiguous increase in electron current due to this mode
 - do these results hold in 2D and 3D?
- Are there significant advantages to considering the physics of this mode in other ways?
 - Vlasov vs PIC, or fluid vs kinetic?
- What is the state of our understanding of the transport mechanism?

Electron cyclotron drift instability (ECDI): experiments

- Measurement with coherent Thomson scattering: electron density fluctuations
 - mode frequencies and length scales matching those predicted in simulations
 - linear, continuous dispersion relation
 - convection of electron density fluctuations beyond the thruster exit plane
 - mode propagation in 3D dimensions: contribution to smoothing of cyclotron resonances
 - propagation within a narrow angular extent
 - Tsikata et al, Phys. Plasmas 16, 033506 (2009); Phys. Plasmas 17, 112110 (2010); Cavalier et al. Phys. Plasmas 20, 082107 (2013)



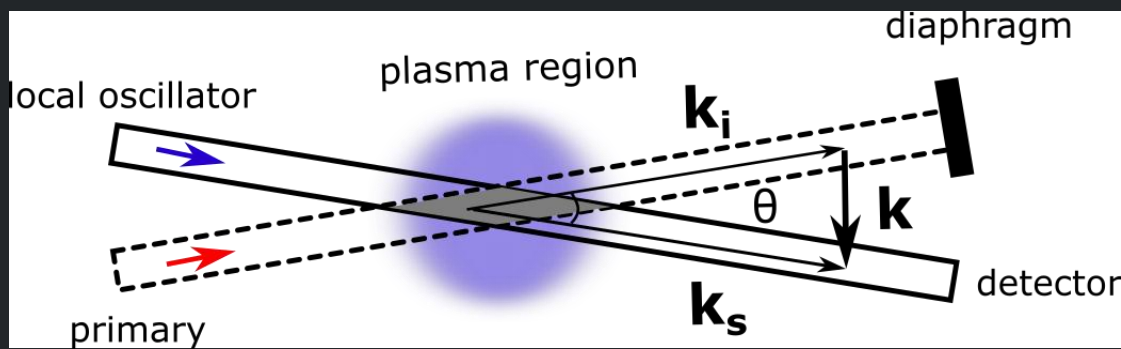
experimental dispersion relation, represented with dynamic form factors: linear and continuous



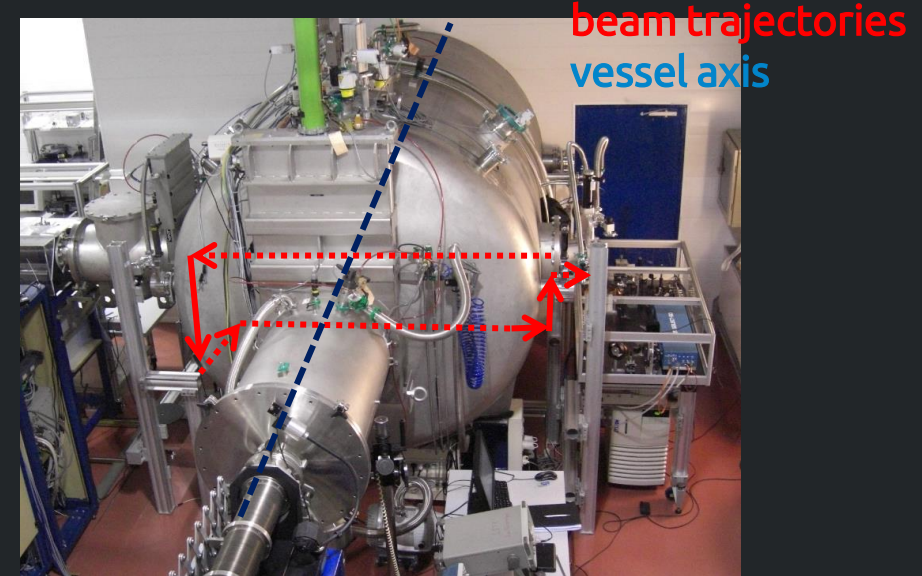
exponential distribution of amplitude with scale

Electron cyclotron drift instability (ECDI): experiments

- Implementation



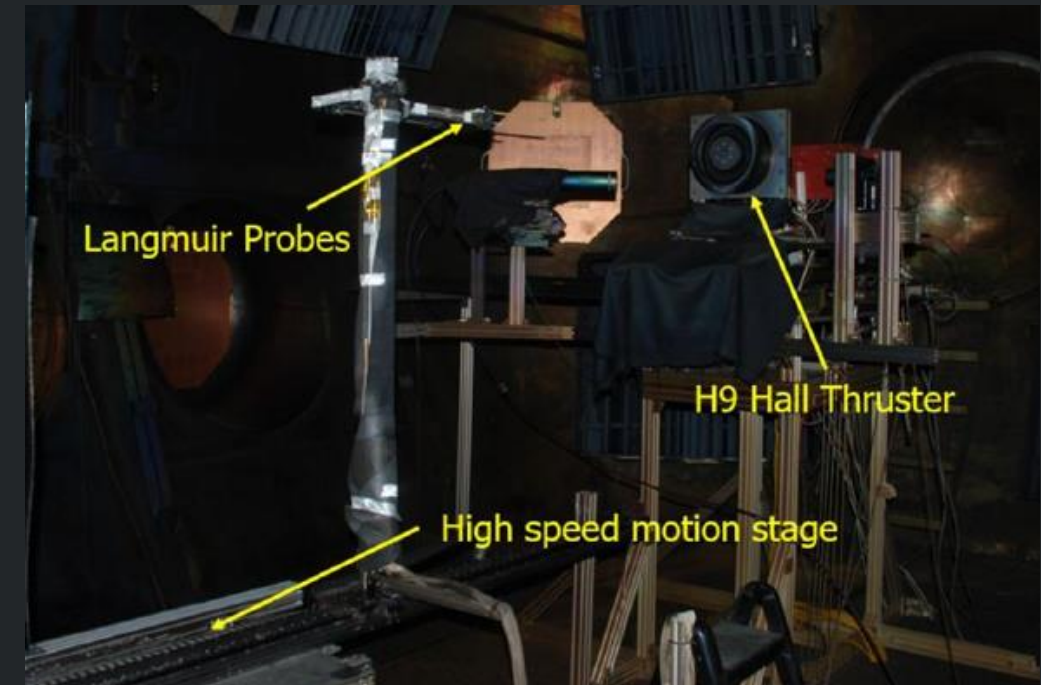
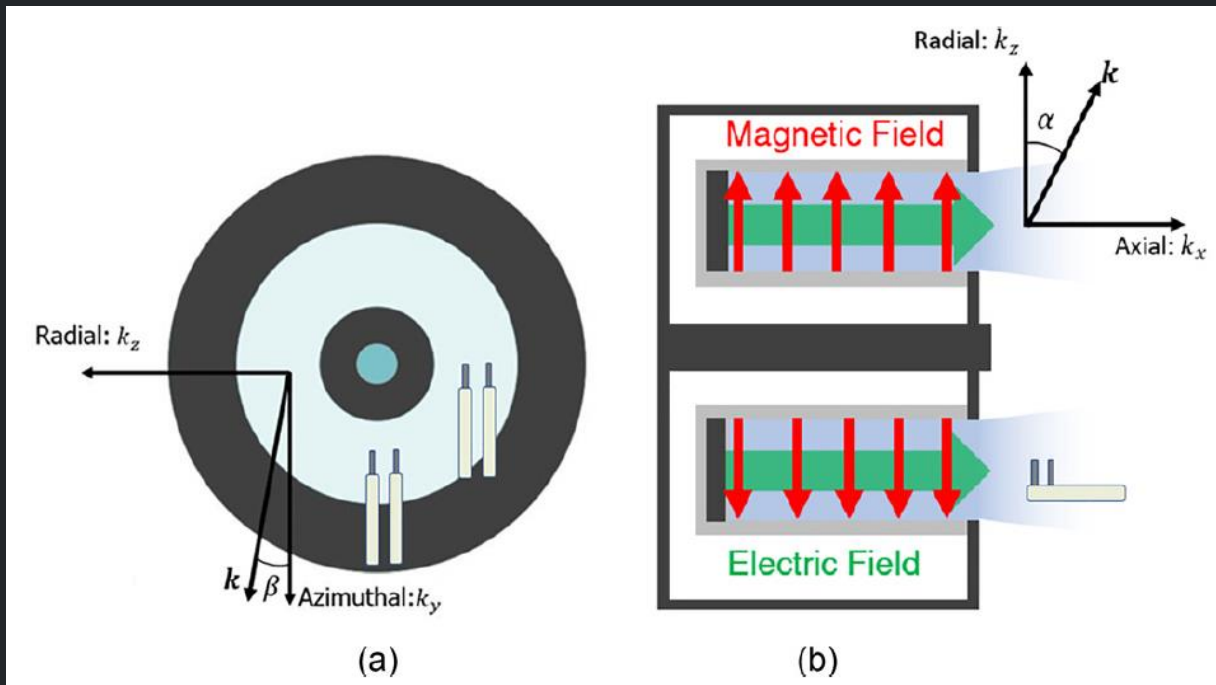
$$\vec{E}_s(\vec{r}, t) \propto \iiint_V e^{-i\vec{k} \cdot \vec{r}} \rho(\vec{r}, t) d^3\vec{r}$$



- direct measurement of electron density fluctuations at length scales of instability
- experiment motivated by numerical simulations showing presence of ECDI (Adam, Héron and Laval 2004)

Electron cyclotron drift instability (ECDI): experiments

- Probe based measurements of fluctuations in thruster channel and near field



Brown and Jorns, Phys. Plasmas 26, 113504 (2019)
Brown and Jorns, AIAA-2021-3415

Electron cyclotron drift instability (ECDI): experiments

- **Technique:** ion saturation probes

- **Analysis methods**

- Cross-correlation between probes to infer wave dispersion
- Quasilinear theory with measured frequency spectrum of oscillations to calculate effective collision frequency

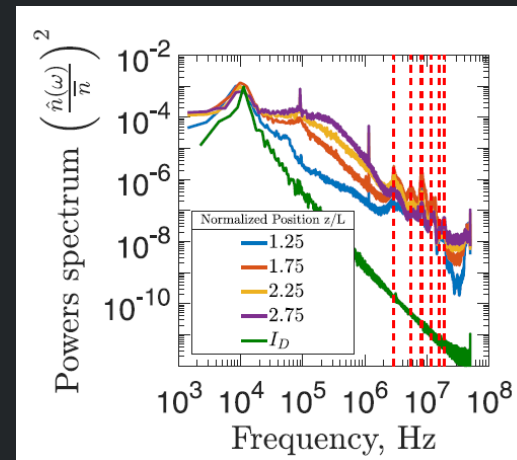
- **Observations**

- Evidence of both cyclotron resonances and ion acoustic features
- Broadband long-wavelength modes downstream
- Evidence of non-linear energy cascade from short to long wavelengths

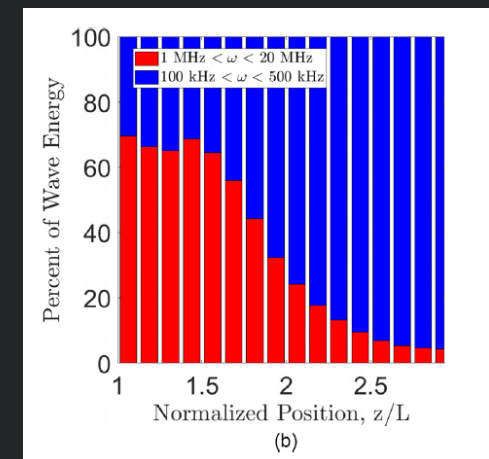
Brown and Jorns, Phys. Plasmas 26, 113504 (2019)

Brown and Jorns, AIAA-2021-3415

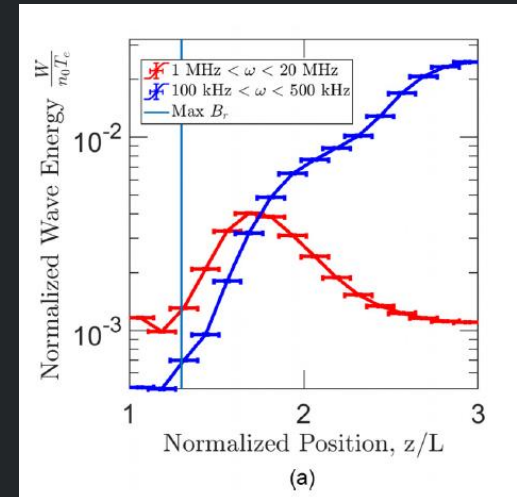
Power spectrum at different axial locations



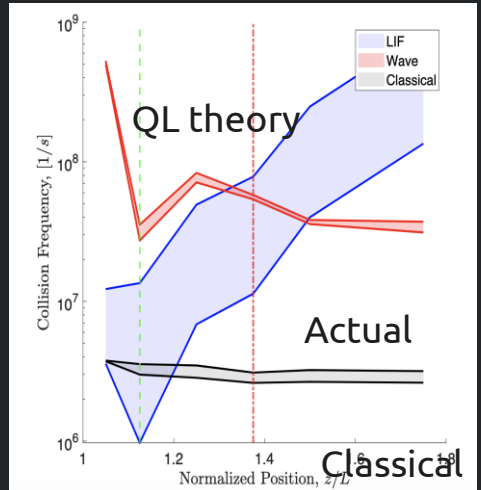
Fraction of energy as function of position



Total energy as function of position



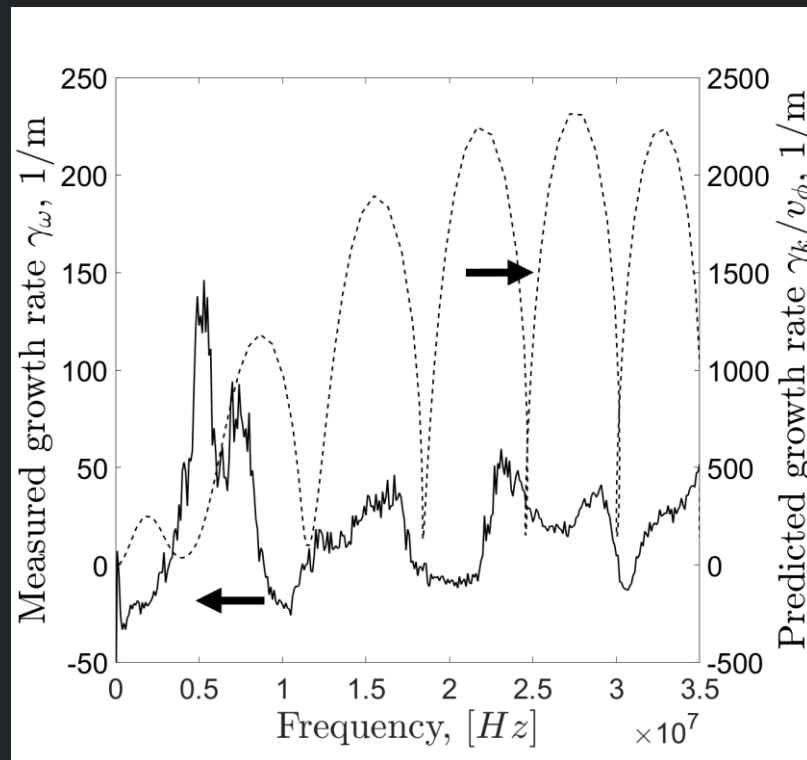
Comparison of effective collision freq.



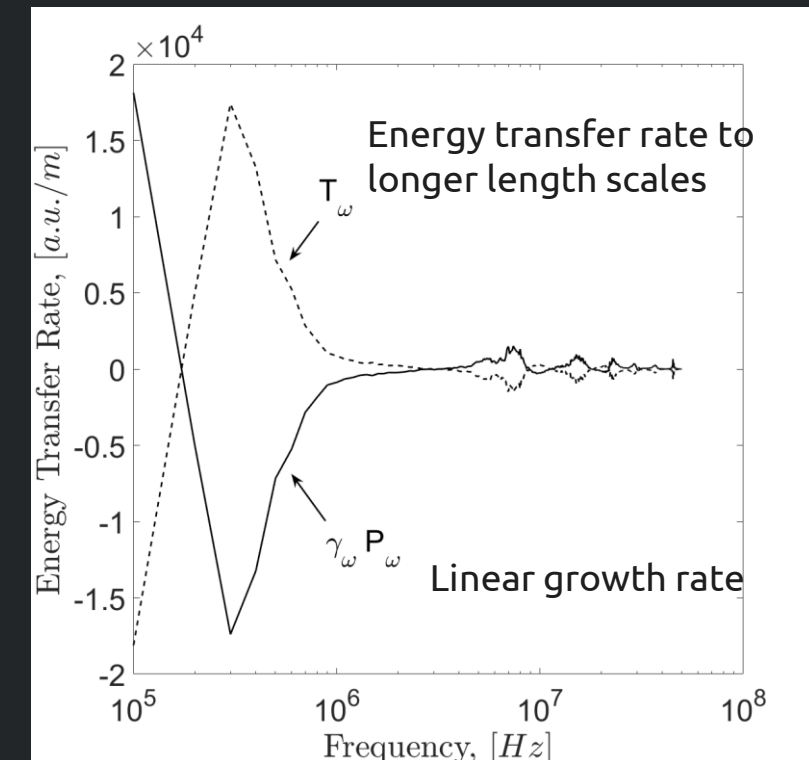
Electron cyclotron drift instability (ECDI): experiments

- **Technique:** ion saturation probes
- **Analysis method:** bispectral calculation between two probes to infer wave-wave interactions and linear growth (Ritz and Kim method)
- **Observations**
 - Measured linear growth of ECDI **does not match** linear theory for growth rate.
 - Energy introduced to waves at cyclotron resonances, transferred across lengthscales to long wavelengths, and dissipated at long wavelengths by collisional or other effects

Measured versus theoretical growth



Linear and non-linear growth



Modified two stream instability (MTSI)
Lower hybrid drift instabilities (LHDI)

Modified two stream instability (MTSI)

MTSI is the lowest-frequency mode of the ECDI family for finite $k_{\parallel} \neq 0$

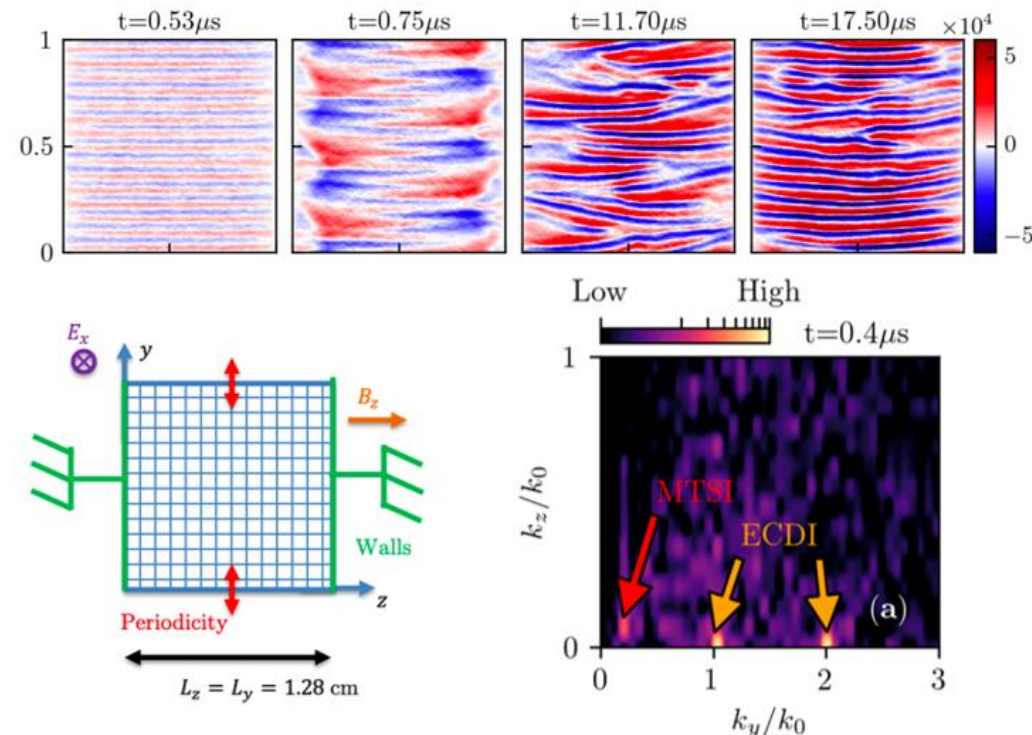
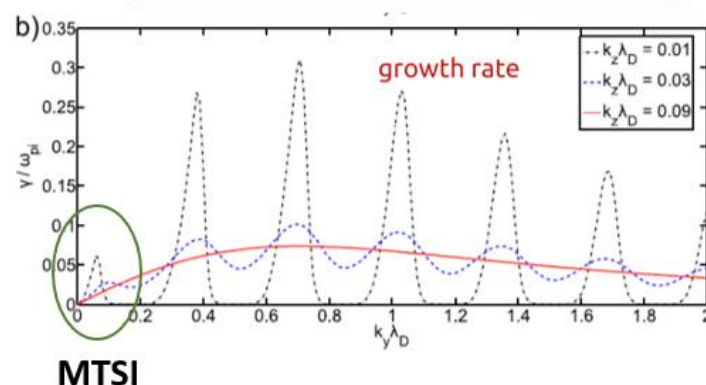
Partially magnetized plasma dispersion relation

$$1 + \frac{1}{k^2 \lambda_D^2} \left[1 + \frac{\omega - k_y V_d}{k_z v_{the} \sqrt{2}} e^{-\gamma} \sum_{m=-\infty}^{+\infty} Z(\zeta_m) I_m(\gamma) \right] - \frac{1}{2k^2 \lambda_{Di}^2} Z' \left(\frac{\omega - k_x v_i}{kv_{thi} \sqrt{2}} \right) = 0$$

MTSI [McBride PoF **15**, 2367 (1972)]

for which $k \rho_e \ll 1$, $k v_i < |\omega - \mathbf{k} \cdot \mathbf{U}|$, and $k_z v_e < |\omega|$ are described by the following simplified dispersion relation^{4-8,10,11}:

$$1 + \frac{k_x^2 \omega_{pe}^2}{k^2 \Omega_e^2} - \frac{\omega_{pi}^2}{(\omega - \mathbf{k} \cdot \mathbf{U})^2} - \frac{k_z^2 \omega_{pe}^2}{k^2 \omega^2} = 0. \quad (5)$$



Coupling between ECDI and MTSI
Villafana et al. PSST **30**, 075002 (2021)

Plasma instabilities in Hall thrusters studied extensively, but mostly near the acceleration zone

- Anomalous transport of electrons in the vicinity of the acceleration zone has dominated investigations of plasma instabilities in Hall thrusters for over three decades [1]

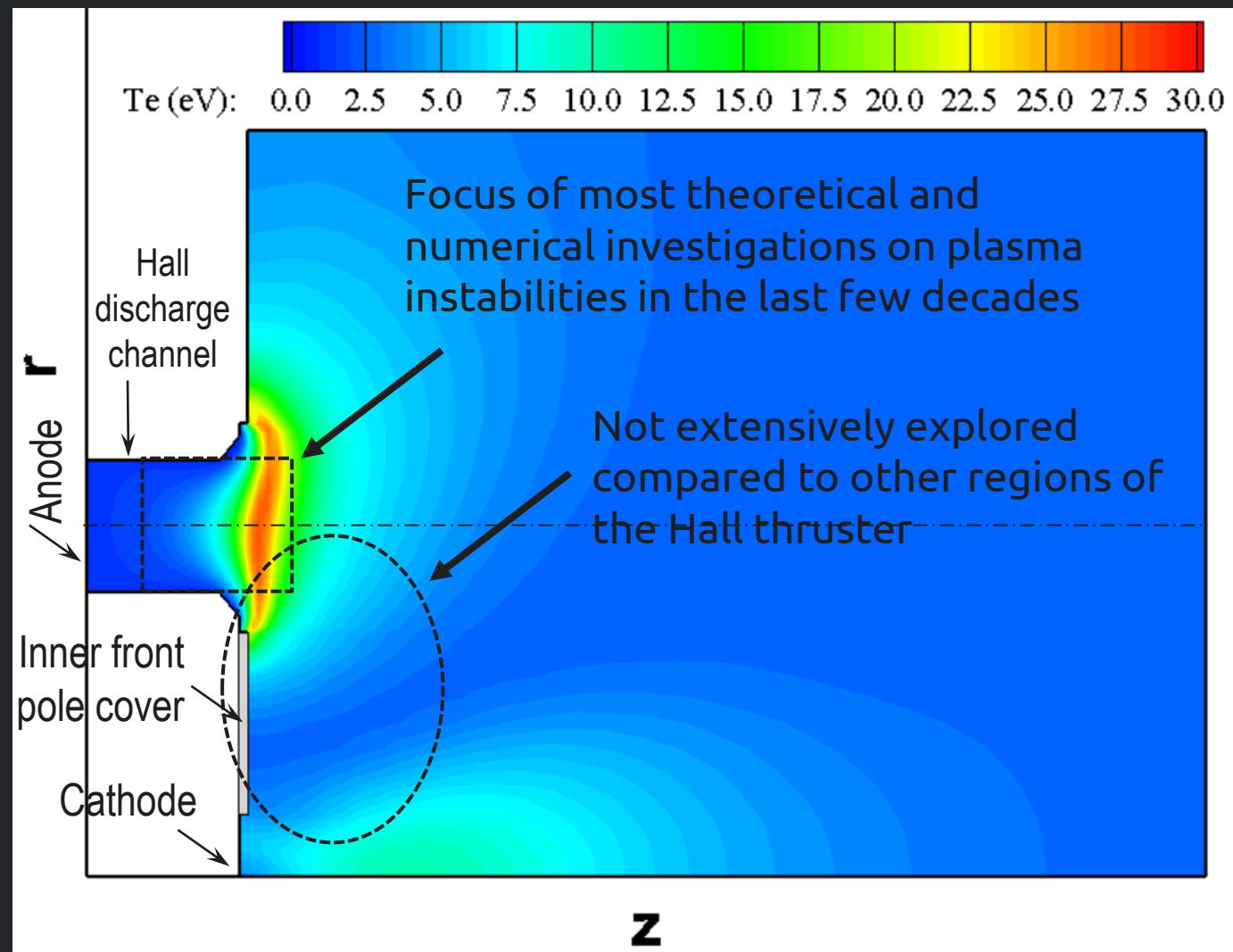
[1] Kaganovich, I. D., *et al.*, "Perspectives on Physics of E×B Discharges Relevant to Plasma Propulsion and Similar Technologies," *Physics of Plasmas*, 27 (2020).

[2] Jorns, B., *et al.*, "Mechanisms for Pole Piece Erosion in a 6-kW Magnetically-Shielded Hall Thruster," AIAA-2016-4839.

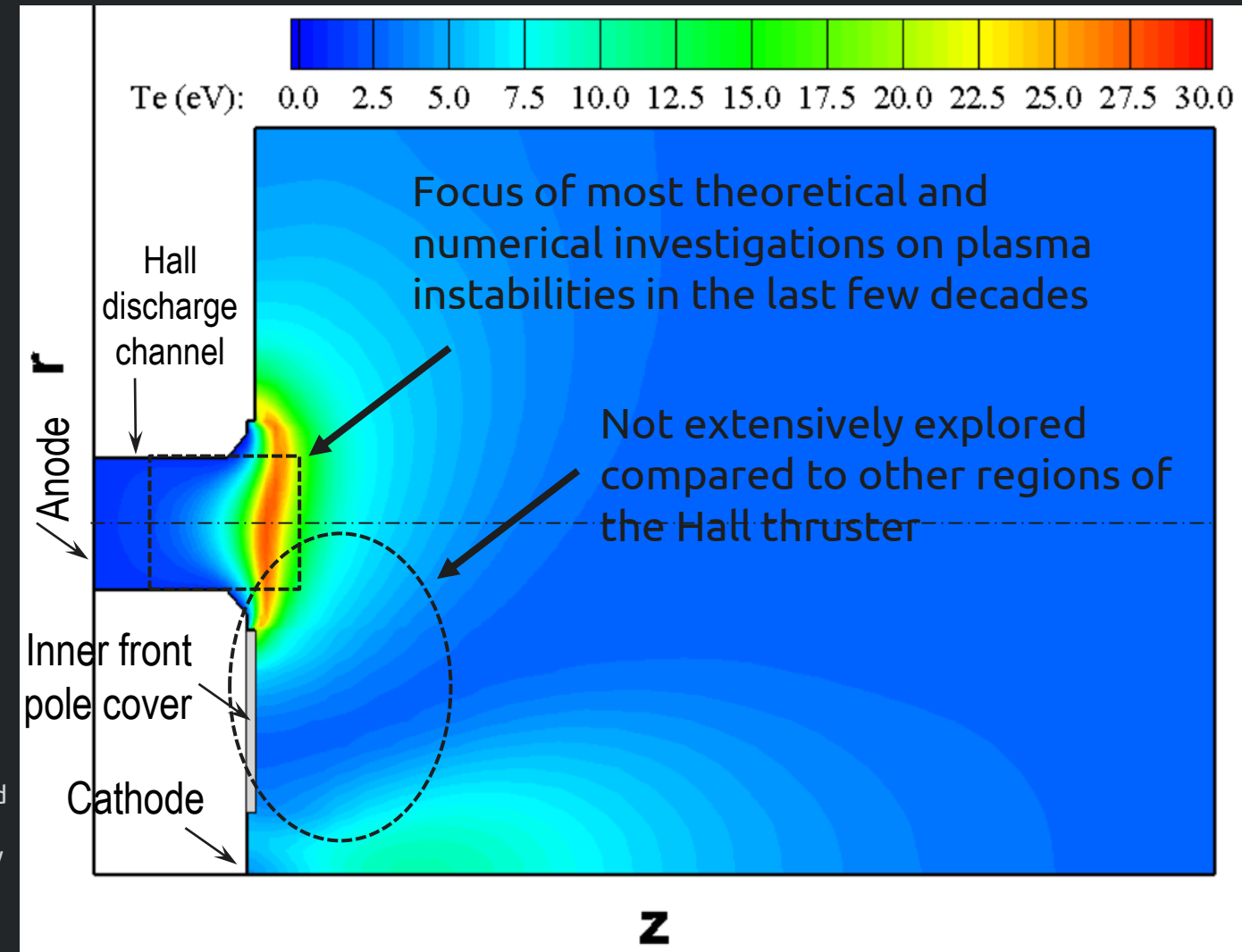
[3] Huang, W., Kamhawi, H., "Counterstreaming Ions at the Inner Pole of a Magnetically Shielded Hall Thruster," *J. Appl. Phys.* 129, (2020).

[4] Huang, W., *et al.*, "Ion Velocity Characterization of the 12.5-kW Advanced Electric Propulsion System Engineering Hall Thruster", AIAA-2021-3432.

Hall2De simulation of HERMeS (300 V, 20.8 A)



- Interest in the plume region between the ion beam and centered-mounted hollow cathode sparked by observations in last decade:
 - low but measurable erosion of the front magnet poles observed in the 6-kW H6MS lab Hall thruster [2] but absent in the unshielded version; observed also in the 12.5-kW HERMeS developed later
 - broad ion velocity distribution functions measured by LIF (effective ion temperatures several to tens of eV if fitted to Maxwellians) [2-4]
 - classical mechanisms could not explain all measurements



[1] Kaganovich, I. D., *et al.*, "Perspectives on Physics of $E \times B$ Discharges Relevant to Plasma Propulsion and Similar Technologies," *Physics of Plasmas*, 27 (2020).

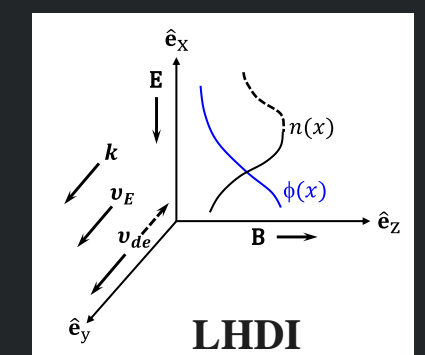
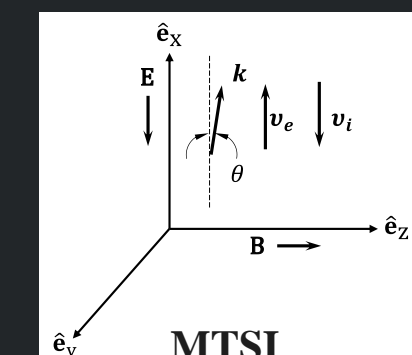
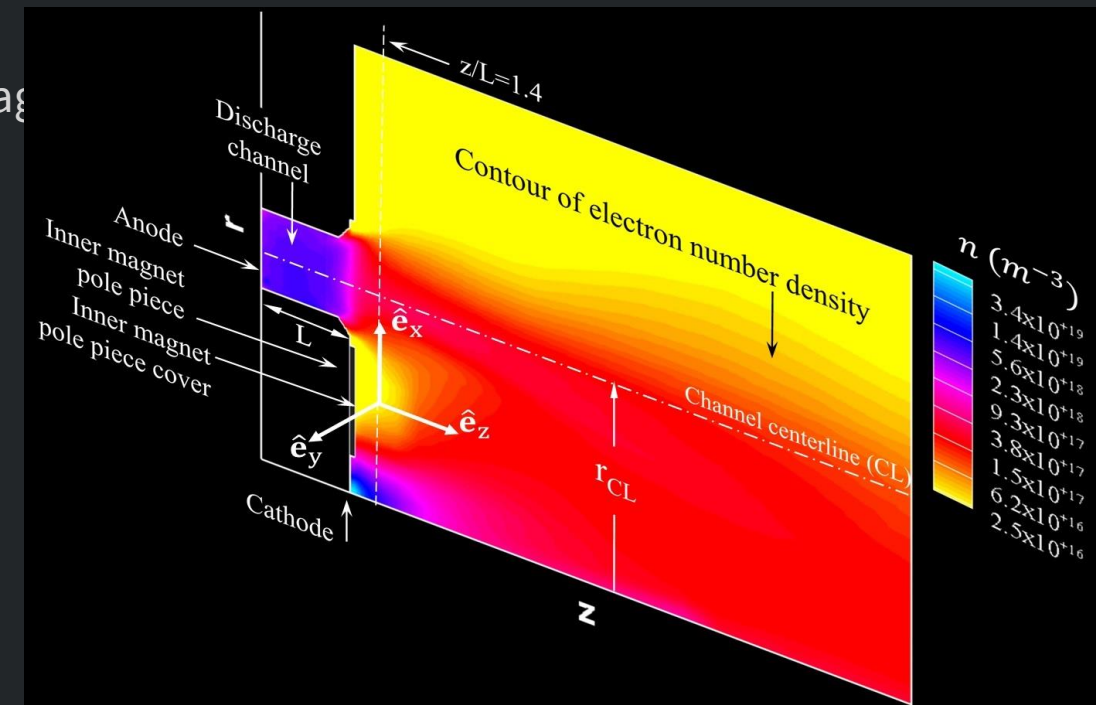
[2] Jorns, B., *et al.*, "Mechanisms for Pole Piece Erosion in a 6-kW Magnetically-Shielded Hall Thruster," AIAA-2016-4839.

[3] Huang, W., Kamhawi, H., "Counterstreaming Ions at the Inner Pole of a Magnetically Shielded Hall Thruster," *J. Appl. Phys.* 129, (2020).

[4] Huang, W., *et al.*, "Ion Velocity Characterization of the 12.5-kW Advanced Electric Propulsion System Engineering Hall Thruster", AIAA-2021-3432.

Instabilities in the Lower-Hybrid (LH) frequency range between the ion beam and hollow cathode first considered at JPL more than a decade ago

- Studied intensely in the 70s and 80s.
 - Laboratory applications: most commonly in z - and θ -pinches.
 - Space applications: conditions in the magneto-sheath and magneto-pause regions.
- Three distinct instabilities received most attention
 - Modified two-stream instability (MTSI): ion beam streaming \perp to \mathbf{B} in a background homogeneous plasma, allowing for $k_{\parallel} \neq 0$. [1]
 - Ion-ion cross-field instability: counter-streaming ions \perp to \mathbf{B} in a homogeneous plasma ($k_{\parallel} = 0$). [2]
 - Lower-hybrid drift instability (LHDI): driven by in-homogeneities (dn/dx , dTe/dx , dB/dx). [3]

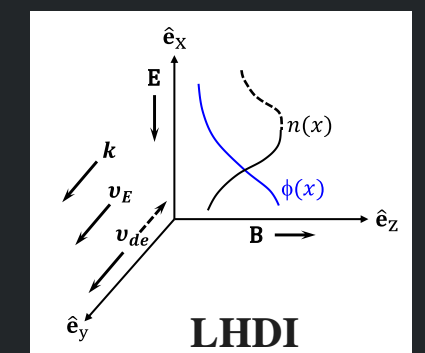
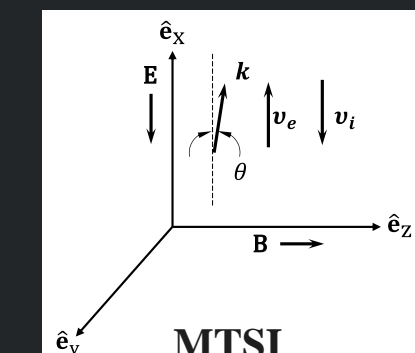
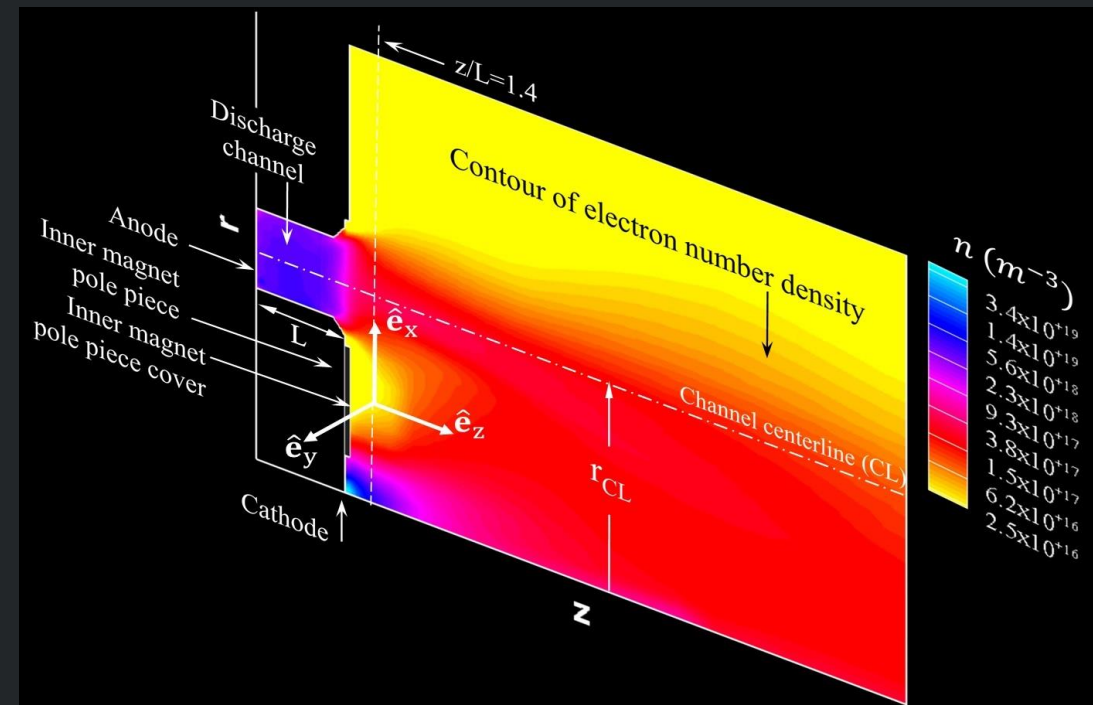


[1] J. B. McBride, E. Ott, J. P. Boris, and J. H. Orens, "Theory and Simulation of Turbulent Heating by Modified 2-Stream Instability," *Physics of Fluids*, vol. 15, no. 12, pp. 2367-2383, 1972.

[2] S. P. Gary, R. L. Tokar, and D. Winske, "Ion Ion and Electron-Ion Cross-Field Instabilities near the Lower Hybrid Frequency," *Journal of Geophysical Research-Space Physics*, vol. 92, no. A9, pp. 10029-10038, Sep 1, 1987.

[3] N. A. Krall, and P. C. Liwer, "Low-Frequency Instabilities in Magnetic Pulses," *Physical Review A*, vol. 4, no. 5, pp. 2094-2104, 1971.

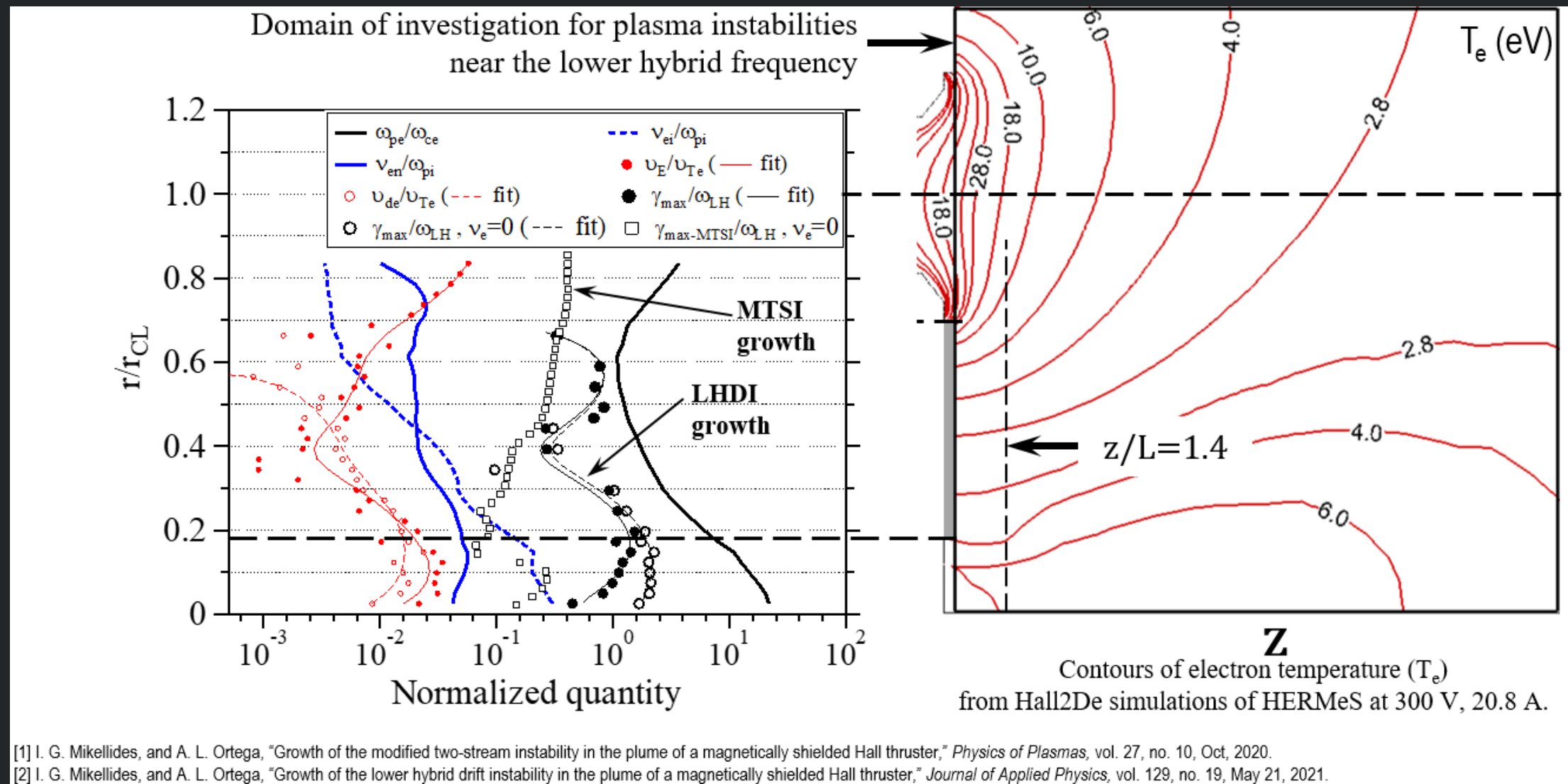
- Notable characteristics
 - Low threshold, relative drift $U \gtrsim (T_i/m_i)^{1/2}$ not $(T_e/m_e)^{1/2}$
 - Not subject to strong ion Landau damping \rightarrow can grow when other electrostatic instabilities cannot.
 - Unlike many electron-ion instabilities which mainly heat electrons, LH instabilities can heat ions anomalously to comparable or even higher temperatures than T_e , \perp to \mathbf{B} .



[1] J. B. McBride, E. Ott, J. P. Boris, and J. H. Orens, "Theory and Simulation of Turbulent Heating by Modified 2-Stream Instability," *Physics of Fluids*, vol. 15, no. 12, pp. 2367-2383, 1972.

[2] S. P. Gary, R. L. Tokar, and D. Winske, "Ion Ion and Electron-Ion Cross-Field Instabilities near the Lower Hybrid Frequency," *Journal of Geophysical Research-Space Physics*, vol. 92, no. A9, pp. 10029-10038, Sep 1, 1987.

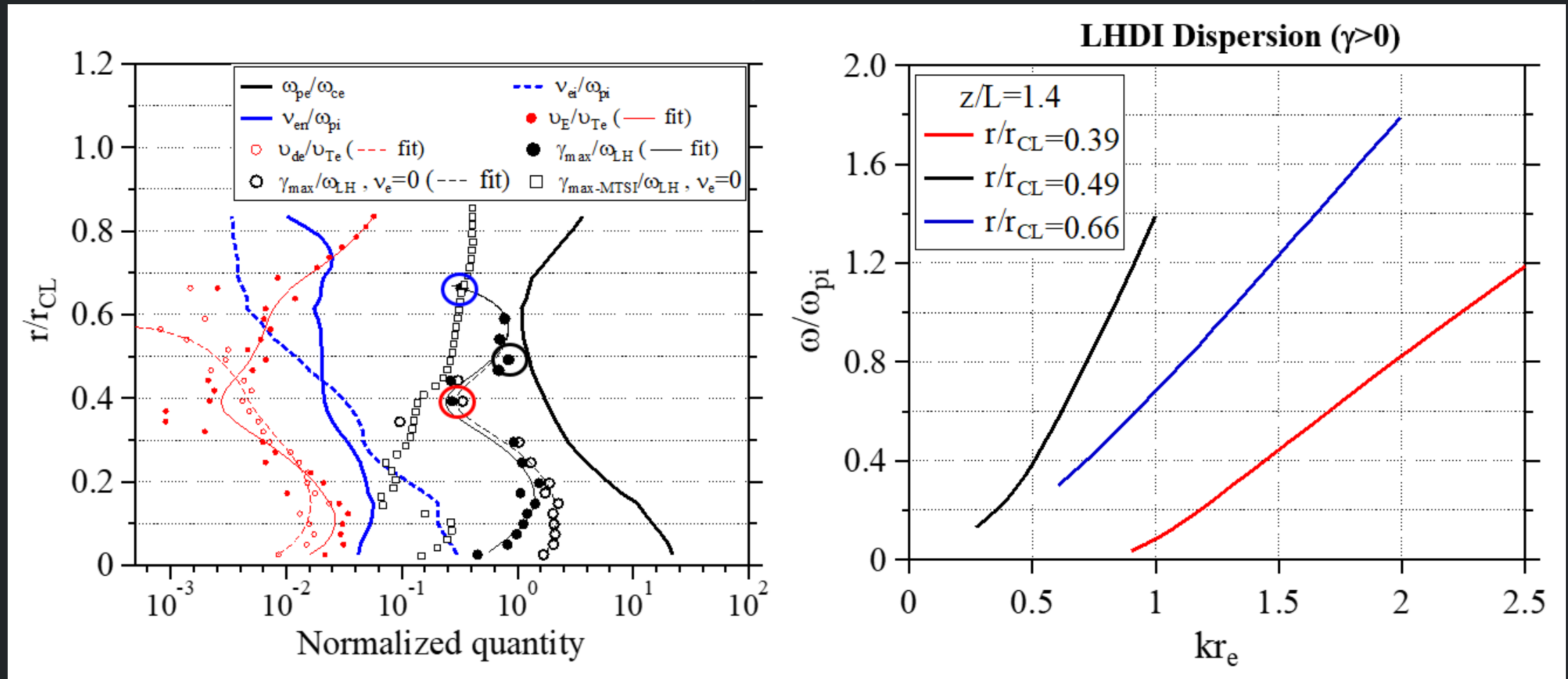
[3] N. A. Krall, and P. C. Liewer, "Low-Frequency Instabilities in Magnetic Pulses," *Physical Review A*, vol. 4, no. 5, pp. 2094-8, 1971.



[1] I. G. Mikellides, and A. L. Ortega, "Growth of the modified two-stream instability in the plume of a magnetically shielded Hall thruster," *Physics of Plasmas*, vol. 27, no. 10, Oct, 2020.

[2] I. G. Mikellides, and A. L. Ortega, "Growth of the lower hybrid drift instability in the plume of a magnetically shielded Hall thruster," *Journal of Applied Physics*, vol. 129, no. 19, May 21, 2021.

Theoretical predictions awaiting direct comparison with ongoing measurements of the wave dispersion in this region



Electrostatic dispersion relation for an unbounded plasma in a fixed magnetic field

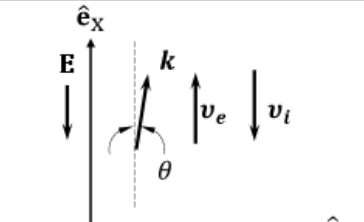
$$1 + \sum_s \chi_s(\mathbf{k}, \omega) = 0$$

Electrostatic dispersion relation ($\beta_e = 2\mu_0 p_e / B^2 = 0$) for an unbounded, plasma consisting of un-magnetized ions ($kr_i \gg 1, |\omega|/\omega_{ci} \gg 1$) and magnetized electrons ($|\omega|/\omega_{ce} \ll 1, k \wedge r_e \lesssim 1$) in a constant magnetic field.

Collisionless homogeneous plasma with small or zero k_z (MTSI)

$$\chi_e(\mathbf{k}, \omega) = \frac{2\omega_{pe}^2}{k^2 v_{Te}^2} \left\{ 1 - e^{-(k_x^2 r_e^2/2)} I_0(\frac{1}{2} k_x^2 r_e^2/2) [1 + \frac{1}{2} Z'(\zeta_e)] \right\} \quad \chi_i(\mathbf{k}, \omega) = -\frac{\omega_{pi}^2}{k^2 v_{Ti}^2} Z'(\zeta_i)$$

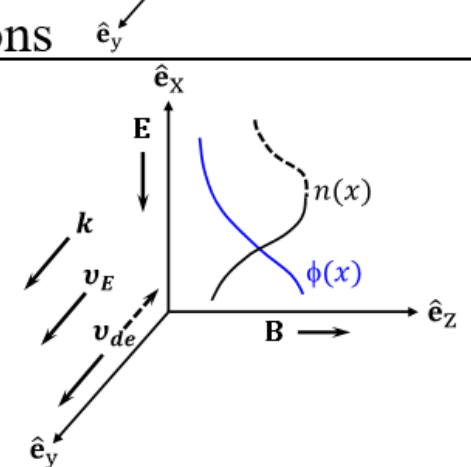
$$\zeta_e = v_{Te}^{-1} \frac{\omega}{k\theta} \quad \zeta_i = v_{Ti}^{-1} \left(\frac{\omega}{k} - v \right) \quad v = |v_e - v_i|$$



Inhomogeneous plasma with $k_y \neq 0$ (LHDI), accounting for electron collisions

$$\chi_e(\mathbf{k}, \omega) = \frac{2\omega_{pe}^2}{k^2 v_{Ts}^2} \left[1 - \frac{(\omega - k_y v_{De}) \varphi_e(\mathbf{k}, \omega')}{1 - i v_e \varphi_e(\mathbf{k}, \omega')} \right] \quad \chi_i(\mathbf{k}, \omega) = -\frac{\omega_{pi}^2}{k^2 v_{Ti}^2} Z'(\zeta_i)$$

$$\varphi_e(\mathbf{k}, \omega') = \sum_{j=-\infty}^{\infty} \frac{\Lambda_{ej}(\lambda_e)}{\omega' + j\omega_{ce}} \quad \Lambda_{ej} \equiv I_j e^{-\lambda_e} \quad \zeta_i = \frac{\omega}{k_y v_{Ti}}$$

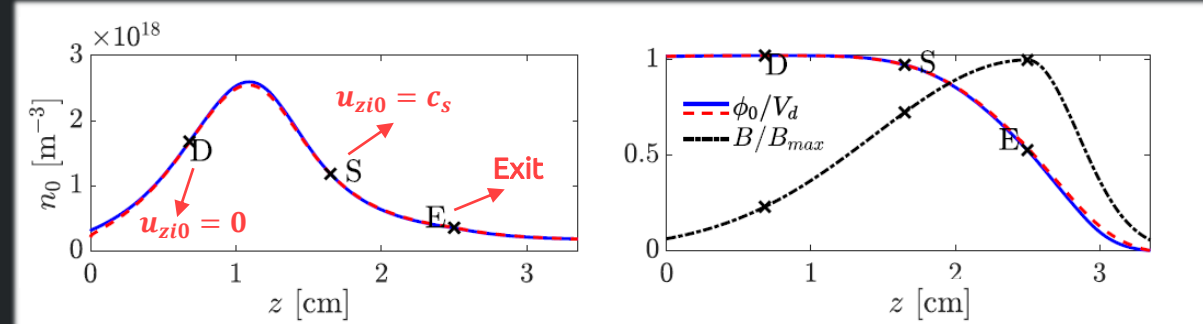


E. Bello-Benítez and E. Ahedo, *Axial-azimuthal, high-frequency modes from global linear-stability model of a Hall thruster*, Plasma Sources Science and Technology, Vol. 30, 2021, pp. 035003.

Model characteristics

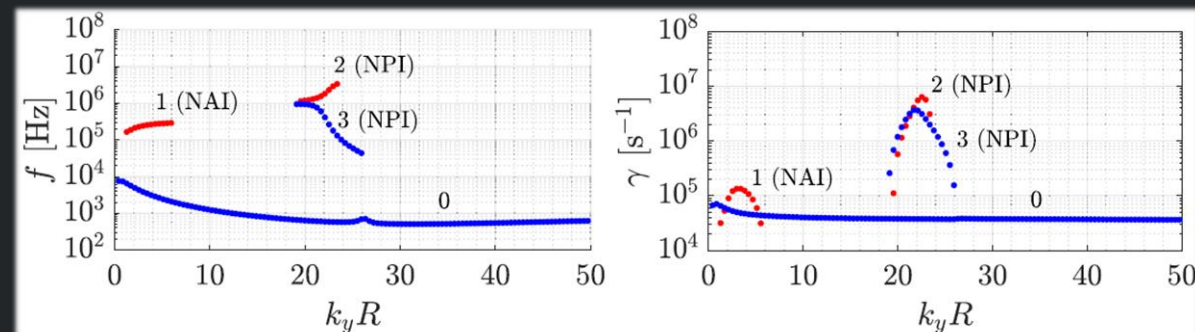
- Two-fluid global linear stability model, consistent with the significant axial inhomogeneity inherent to the Hall discharge.
- Perturbation solutions in the 2D axial-azimuthal plane.
- The perturbation model is applied to an equilibrium solution obtained from a three-fluid 1D-axial model (more information in the corresponding poster session).
- The model fully accounts for the effects of electron pressure and inertia on plasma perturbations (including boundary conditions).
- The unstable mode shapes and ω for each k_y are obtained as solutions to a Sturm Liouville problem.

Equilibrium solution



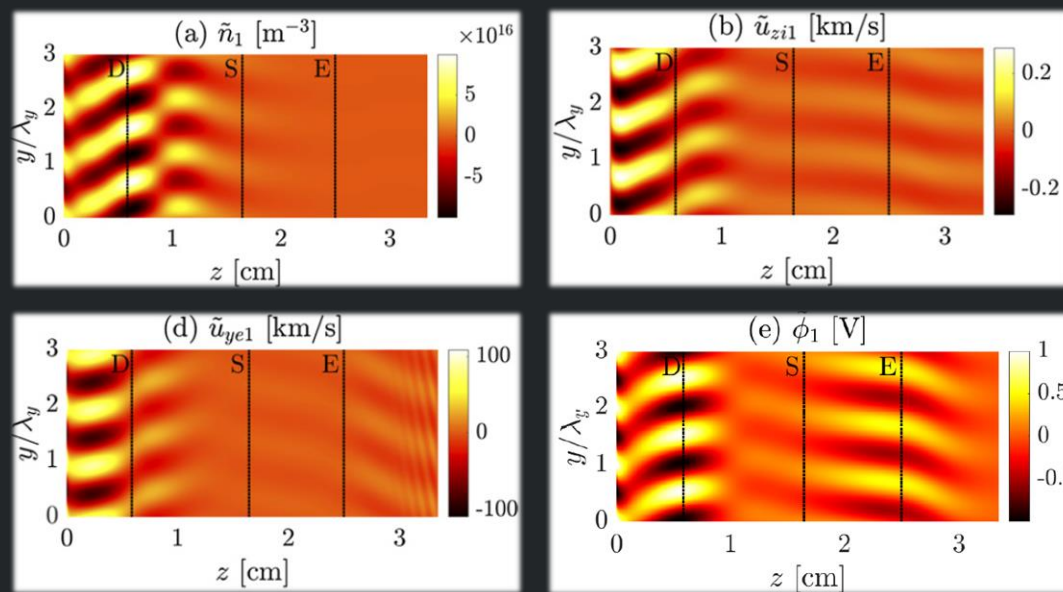
Dispersion relation

For reference case with $T_{e1} = 0$ and equilibrium without electron inertia



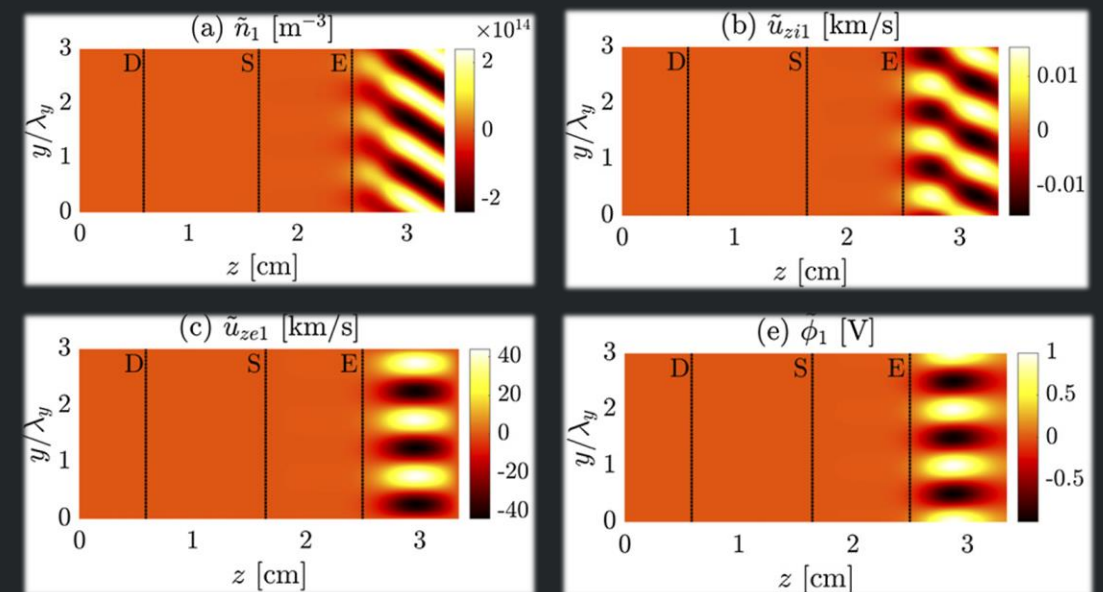
- Mid-frequency sub-dominant near-anode mode moving in the +ExB direction (branch 1).
- Two counter-streaming near-plume modes (branches 2 and 3). The one moving in the +ExB direction dominates (branch 2).

The subdominant near-anode instability (NAI)



- Frequency of 241 kHz.
- Wavelength of 8.90 cm ($k_y R \sim 3$).
- Intense perturbation on electrons and ions.
- Quite sensitive to geometrical and operation parameters.
- Under parametric changes, trends are similar to rotating spokes, as reported by, e.g., Boeuf (2017), Escobar and Ahedo (2015).
- Similarities with drift-gradient instabilities of recent global and local analyses of Sorokina, Marusov *et al* (2019).

The dominant near-plume instability (NPI)



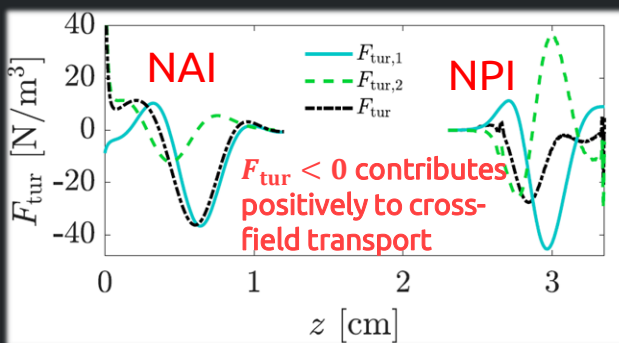
- Frequency of 2.87 MHz.
- Wavelength 1.16cm ($k_y R \sim 23$). Electron perturbations much more intense.
- The region with fluctuations strongly correlates to the region with negative magnetic gradient $dB/dz < 0$.
- Thus, possibly related to local drift-gradient instabilities in, e.g., Ramos *et al* (2021) and Lakhin *et al* (2018).
- Quite robust to changes in geometrical and operation parameters.

Turbulent force

The average in θ and t of perturbed equations (keeping quadratic terms) leads to the expression of the turbulent force $F_{\text{tur}} = F_{\text{tur},1} + F_{\text{tur},2}$, with:

- Electric force: $F_{\text{tur},1} = -e\langle\tilde{n}_1\tilde{E}_{y1}\rangle$
- Inertial force: $F_{\text{tur},2} = -m_e \left[\left\langle \tilde{n}_1 \frac{\partial \tilde{u}_{ye1}}{\partial t} \right\rangle + \frac{\partial u_{ye0}}{\partial z} \langle \tilde{n}_1 \tilde{u}_{ze1} \rangle + n_0 \left\langle \tilde{u}_{ze1} \frac{\partial \tilde{u}_{ye1}}{\partial z} \right\rangle + \langle \tilde{n}_1 (\mathbf{u}_0 \cdot \nabla) u_{ye1} \rangle \right]$
- For the NAI, the pressure contribution dominates.
- For the NPI, both inertia and pressure are equally important.
- F_{tur} contributes globally in a positive way to cross-field transport.
- F_{tur} is axially rippled and locally $F_{\text{tur}} > 0$ is found in some subregions, which goes against cross-field transport.

Perturbations scaled so that NPI and NAI F_{tur} compensates the magnetic force in their respective regions



Conclusion

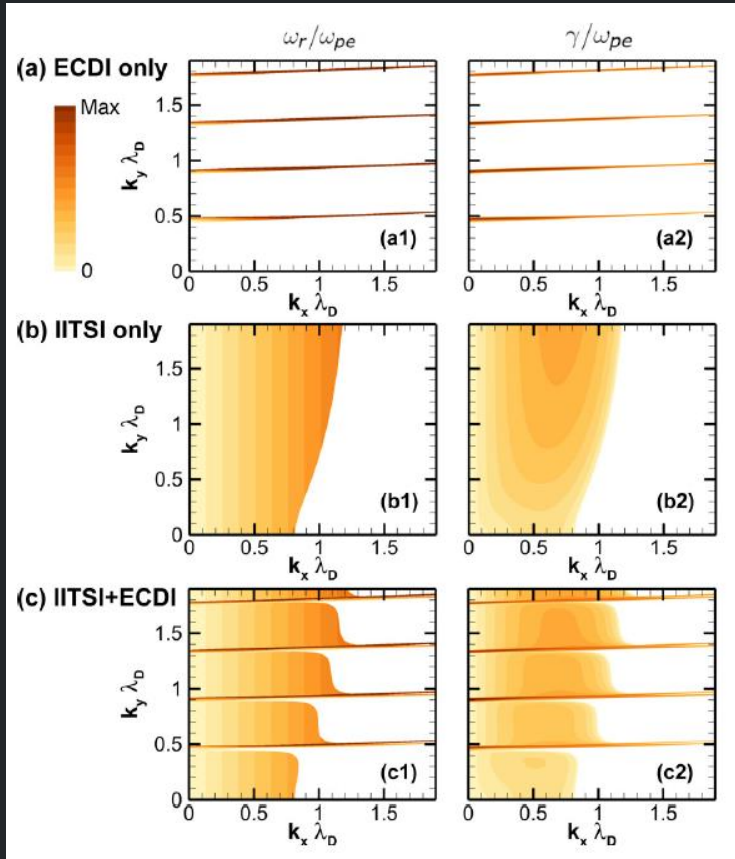
- Global stability analysis focused on the mid-to-high frequency range.
- Two well-characterized modes:
 - Dominant near-plume instability (NPI) with $f \sim 1\text{-}30$ MHz and $k_y R \sim 10\text{-}40$.
 - Sub-dominant near-anode instability (NAI) with $f \sim 100\text{-}300$ kHz and $k_y R \sim 1\text{-}10$.
- Accounting for T_{e1} or 0th order electron inertia may lead to new higher-frequency NPI modes.
- Apart from the electric contribution to F_{tur} , the inertial one may be significant for some modes.

Future work

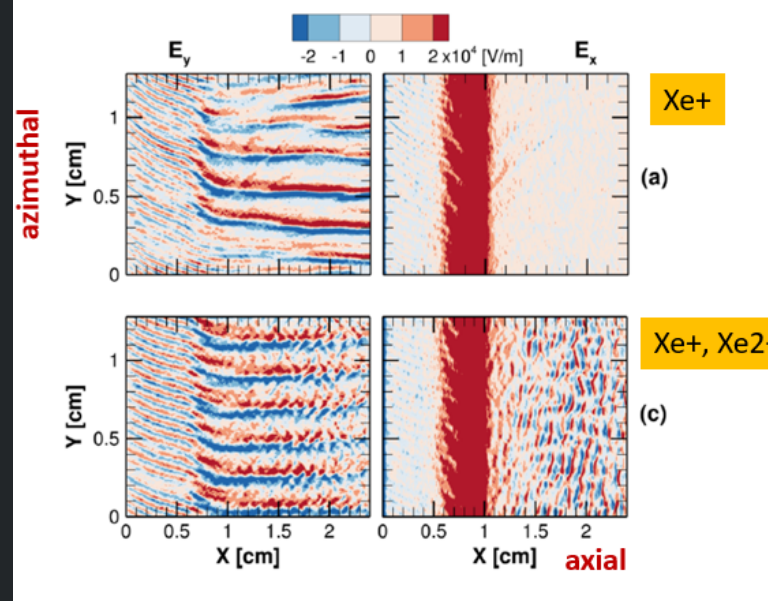
- Further investigate the role of T_{e1} and 0th order electron inertia on instabilities.
- Stability analysis on a larger domain including the plume past the cathode.
- Investigate the influence on NPI.

Ion-ion two stream instability (IITSI)

Another short-scale wave is found (axial) when presence of multiple ion species is taken into account

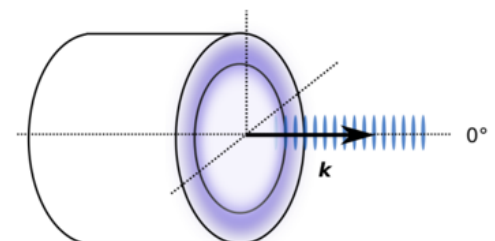


Identification of the ion-ion two stream instability in Hall thrusters



Tsikata et al., Phys. Plasmas 21, 072116 (2014):
measurement and theoretical description

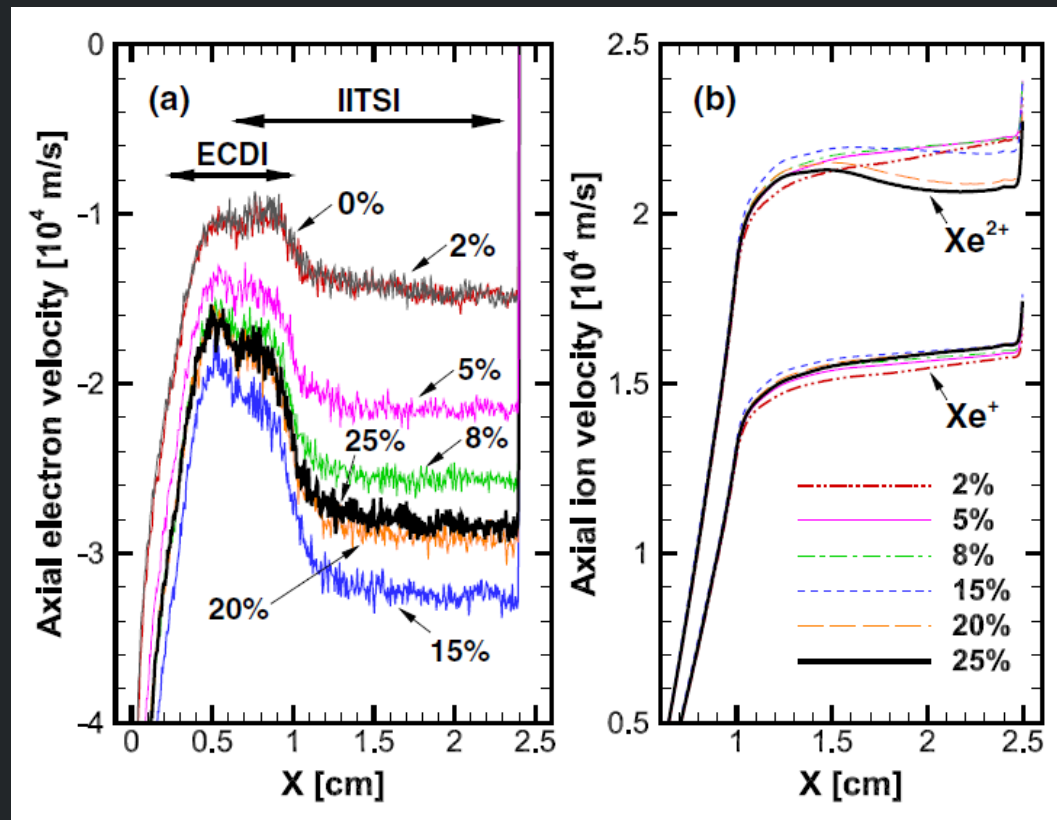
Hara and Tsikata, Phys. Rev. E 102, 023202 (2020):
numerical simulation confirmation



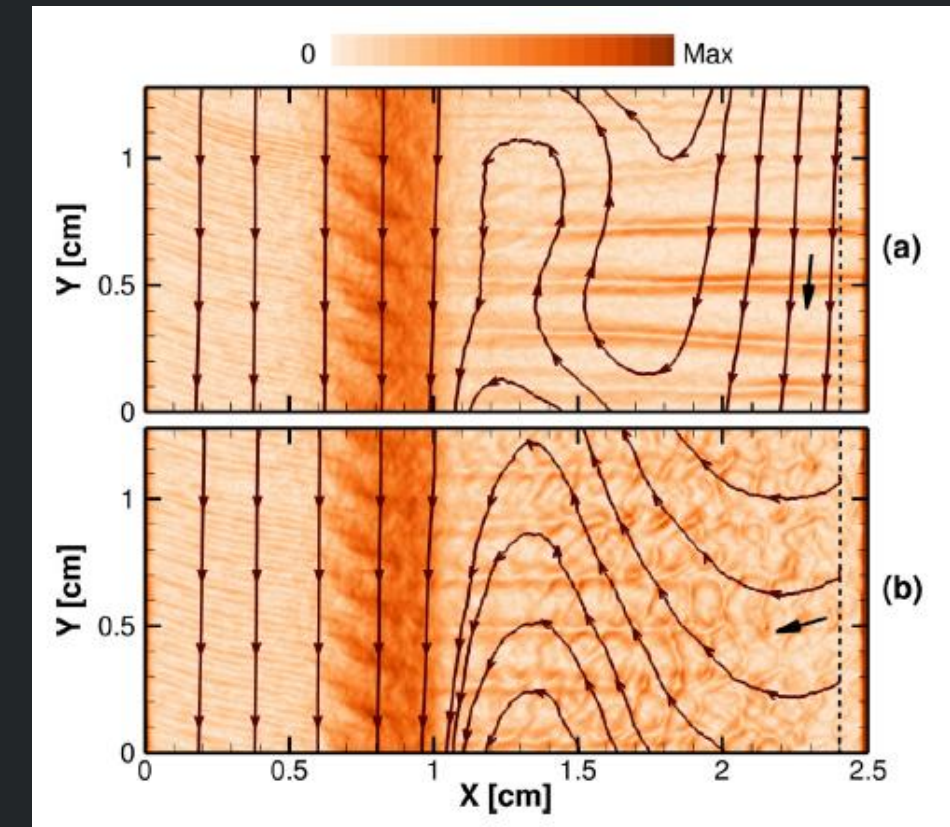
$$(k_{\perp} \lambda_D)^2 \left[1 - \frac{(1 - \alpha) \omega_{pi}^2}{(\omega - \mathbf{k} \cdot \mathbf{U}_i^+)^2} - \frac{\alpha \omega_{pi}^2}{(\omega - \mathbf{k} \cdot \mathbf{U}_i^{2+})^2} \right] + 1 - I_0(b) \exp(-b) + \sum_{n=1}^{\infty} \frac{2\omega^2 I_n(b) \exp(-b)}{(n\omega_B)^2 - \omega^2} = 0 \quad \text{dispersion relation}$$

singly charged⁺ doubly charged²⁺ magnetized electrons

Doubly charged ion fraction: $\alpha = \frac{2n_i^{2+}}{n_e}$



enhanced electron transport in the presence of the IITSI



visualization of electron trajectories

Fluctuation-based electron transport

- Waltz, Phys. Fluids 25, 1269 (1982)
- Liewer, Nucl. Fusion 25, 543 (1985)

$$\langle \Gamma_{ex} \rangle = \frac{\langle n'_e E'_y \rangle}{B_z}$$

$$\langle \Gamma_{ey} \rangle = -\frac{n_{e0} E_{x0}}{B_z} - \frac{\langle n'_e E'_x \rangle}{B_z}$$

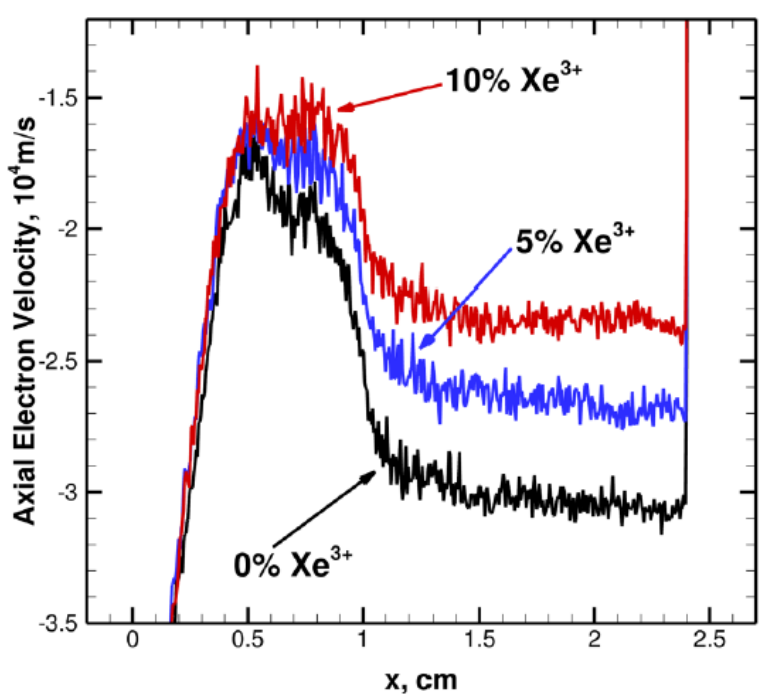


FIG. 4. Cross-field electron transport is reduced when increasing triply charged ion species fraction. Plasma properties are averaged in the y direction and over $5\mu\text{s}$ from $t = 15\text{--}20\mu\text{s}$. For all cases, $\alpha_d = 20\%$ is used, and the results for $\alpha_t = 0\%$, 5%, and 10% are shown.

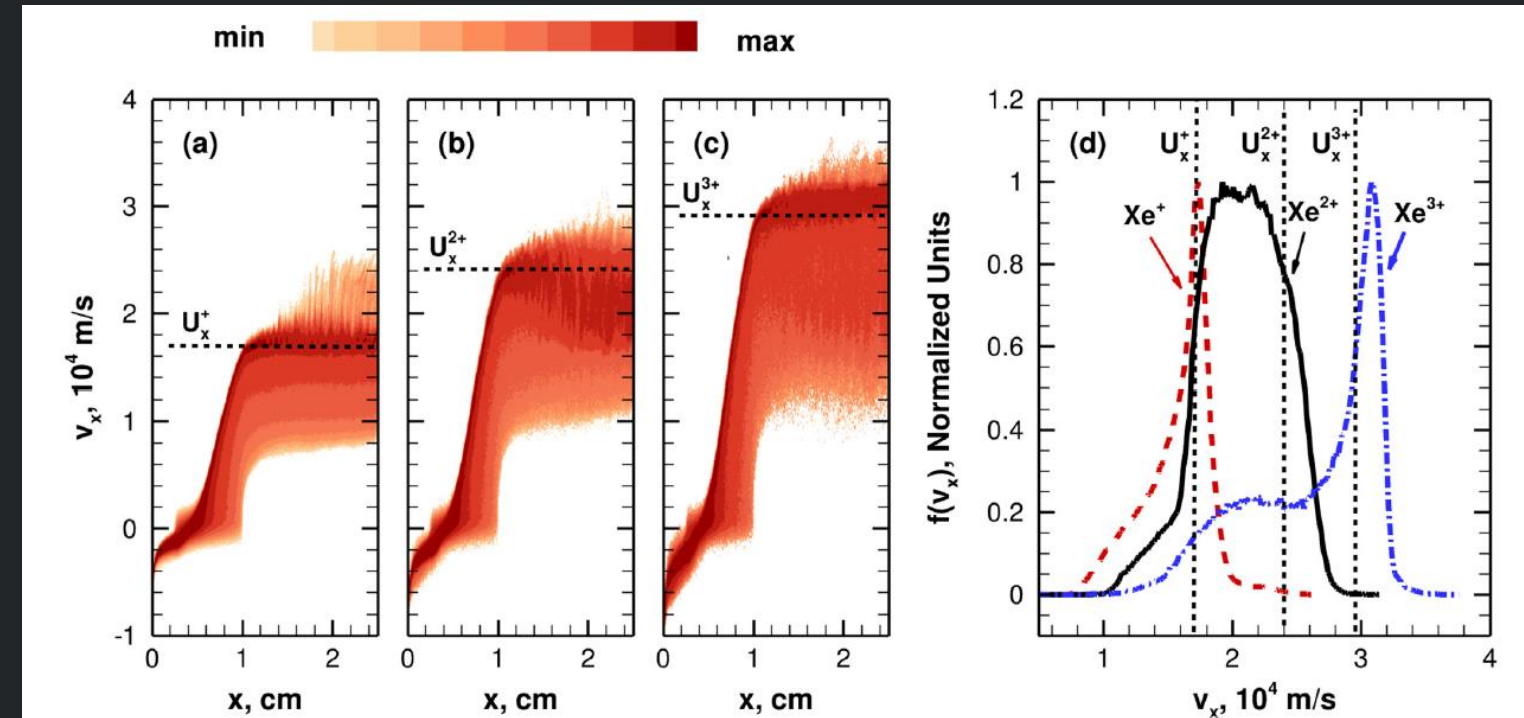


FIG. 5. Instantaneous ion velocity distribution function (IVDF) for the x -component (axial) of the velocity, averaged in the y direction is shown for (a) Xe^+ , (b) Xe^{2+} , and (c) Xe^{3+} . The horizontal dashed lines indicate the ion bulk velocities assuming that the ions are accelerated across a constant voltage drop of 200 V. The colormap shows the VDFs normalized with the reference VDF values, which is chosen as f_{max}^+ for Xe^+ , $0.1f_{\text{max}}^+$ for Xe^{2+} , and $0.01f_{\text{max}}^+$ for Xe^{3+} where f_{max}^+ is the maximum value of Xe^+ VDF. Colorbar uses a logarithmic scale, where min and max correspond to 1.0×10^{-4} and 1.0, respectively. Shown in (d) are the axial VDFs in the plume ($2.0 \leq x \leq 2.3\text{ cm}$) for the three species.

Discussion topics

- What are the key properties we need to measure experimentally in order to relate instabilities to transport? Have we been able to measure these? If not, what are limitations in diagnostic capabilities that have prevented us from measuring them directly?
- What is a summary of what we know experimentally about the instabilities, e.g. spectral shape, growth rate, dispersion? With current experimental capabilities, is there evidence that micro-instabilities can explain anomalous transport?
- What processes lead to the shape of the observed spectra - is it classical turbulence with a forward energy cascade or some other process like an inverse energy cascade?
- How do the waves saturate? What experimental evidence is there for these saturation effects? If there isn't any, how could we measure these?
- How does mode coupling revise we account for the role of individual modes in transport? Ideally, would simulations need to capture all modes?
- 3D simulations vs 2D: is it necessary to hold off on inferences made on the basis of existing codes?
 - dominant length scale vs range
 - inverse cascade

Discussion topics

- Some simulations show the spectrum of instabilities should be ion acoustic like while others show the spectrum should be dominated by cyclotron resonances. Recent experimental evidence seems to suggest that resonances do exist, possibly supporting the latter interpretation. How do we reconcile experiment and simulation if this is the case? Are some simulations overly constrained in terms of dimensions? Is the use of a fixed ionization profile in many simulations the issue? Intriguingly, there was a recent paper that suggested the resonances appear in simulations if the ECDI can couple to an ion transit instability. Is this in keeping with your work on the role of different charge states?